OPTIMAL ACCOMMODATION OF DERs IN PRACTICAL RADIAL DISTRIBUTION FEEDER FOR TECHNO-ECONOMIC AND ENVIRONMENTAL BENEFITS UNDER LOAD UNCERTAINTY CONDITION

Abdulbari Ali Mohamed FREI

2022
PhD THESIS
ELECTRICAL AND ELECTRONICS ENGINEERING

Thesis Advisor
Assoc. Prof. Dr. Muhammet Tahir GÜNEŞER

OPTIMAL ACCOMMODATION OF DERs IN PRACTICAL RADIAL DISTRIBUTION FEEDER FOR TECHNO-ECONOMIC AND ENVIRONMENTAL BENEFITS UNDER LOAD UNCERTAINTY CONDITION

Abdulbari Ali Mohamed FREI

T.C.
Karabuk University
Institute of Graduate Programs
Department of Electrical and Electronics Engineering
Prepared as
PhD Thesis

Thesis Advisor
Assoc. Prof. Dr. Muhammet Tahir GÜNEŞER

KARABUK
October 2022

I certify that in my opinion the thesis submitted by Abdulbari Ali Mohamed FREI titled "ACCOMMODATION OF DERs IN PRACTICAL RADIAL DISTRIBUTION FEEDER FOR TECHNO-ECONOMIC AND ENVIRONMENTAL BENEFITS UNDER LOAD UNCERTAINTY CONDITION" is fully adequate in scope and in quality as a thesis for the degree of PhD.

Assoc. Prof. Dr. Muhammet Tahir GÜNEŞER ....
Thesis Advisor, Department of Electrical and Electronics Engineering

This thesis is accepted by the examining committee with a unanimous vote in the Department of Electrical and Electronics Engineering as a PhD thesis. October 14, 2022

Examining Committee Members (Institutions)		Signature
Chairman	: Prof. Dr. Mehmet KARALI (NEU)	....
Member	: Assoc. Prof. Dr. Muhammet Tahir GÜNEŞER (KBU)	....
Member	: Prof. Dr. Necmi Serkan TEZEL (KBU)	....
Member	: Prof. Dr. Ziyodulla YUSUPOV (KBU)	....
Member	: Assoc. Prof. Dr. Abdülsamed TABAK (NEU)	....

The degree of PhD by the thesis submitted is approved by the Administrative Board of the Institute of Graduate Programs, Karabuk University.

Prof. Dr. Hasan SOLMAZ ....
Director of the Institute of Graduate Programs

"I declare that all the information within this thesis has been gathered and presented in accordance with academic regulations and ethical principles and I have according to the requirements of these regulations and principles cited all those which do not originate in this work as well."

Abdulbari Ali Mohamed FREI

ABSTRACT

Ph. D. Thesis

ACCOMMODATION OF DERS IN PRACTICAL RADIAL DISTRIBUTION FEEDER FOR TECHNO-ECONOMIC AND ENVIRONMENTAL BENEFITS UNDER LOAD UNCERTAINTY CONDITION

Abdulbari Ali Mohamed FREI

Karabük University
Institute of Graduate Programs
The Department of Electrical and Electronics Engineering

Thesis Advisor:
Assoc. Prof. Dr. Muhammet Tahir GÜNEŞER
October 2022, 89 pages

The electricity industry in recent years, with the implementation of incentive policies, has witnessed unprecedented growth in the use of distributed energy resources (DERs) on a small scale and more based on renewable energy. Due to this, in the energy sector, extensive efforts have been made to develop technologies and methods related to the more economical and safer use of renewable energy sources and their connection to power systems. To ensure optimal energy consumption in microgrids (MG), providing a proper and efficient energy management system is of particular importance. By using the receiving energy sources as well as the energy-generating systems in MG, it decreases the amount of pollution caused by the consumption of fossil fuels and gives the reliability of the power system.

This thesis discusses the best possible incorporation of various DERs such as Wind Turbine Generation Systems (WTGS), Electric Vehicles (EVs), Photovoltaic Generation Systems (PVGGS), and Biomass in distribution networks at the same time to reduce overall expense, pollution dispatched by thermal generators, and total grid power loss. A multiple goal function is structured to achieve these planned goals and benefits. Different computational models of DERs were used in this study to analyze the impact on the distribution energy system under varying load demand over a 24-hour period. Furthermore, the discharging/charging model of electric cars at off-peak/peak hours of the distributed grid has been taken into consideration. Because of its robustness, the multi objective crow search algorithm is used to optimize the non-bulgy and non-continuous optimization of the distributed energy grid.

Key Words : Distribution System, Distributed Energy Resources, Emission, Crow Search Algorithm, load uncertainty, Power Loss, Voltage deviation.

Science Code : 90544

ÖZET

Doktora Tezi

BELİRSİZ YÜK KOŞULLARI ALTINDA DAĞITIK YENİLENEBİLİR ENERJİ SİSTEMLERİ OPTİMUM YERLEŞİMİNİN PRATİK RADİAL DAĞILIM BESLEYİCİ İLE TEKNO-EKONOMİK VE ÇEVRESEL FAYDA ANALİZİ

Abdulbari Ali Mohamed FREI

Karabük Üniversitesi
Lisansüstü Eğitim Enstitüsü
Elektrik-Elektronik Mühendisliği

Tez Danışmanı:
Doç. Dr. Muhammet Tahir GÜNEŞER
Ekim, 2022 89 sayfa

Son yıllarda, teşvik politikalarının uygulanmasıyla elektrik sektörü, dağıtık enerji kaynaklarının (DER'ler) küçük ölçekte ve daha çok yenilenebilir enerjiye dayalı kullanımında eşi görülmemiş bir büyümeye tanık olmaktadır. Bu nedenle enerji sektöründe yenilenebilir enerji kaynaklarının daha ekonomik ve güvenli kullanımı ve güç sistemlerine bağlanması ile ilgili teknolojiler ve yöntemler geliştirmek için yoğun çabalar sarf edilmektedir. Mikro şebekelerde (MG) optimum enerji tüketimini sağlamak için uygun ve verimli bir enerji yönetim sistemi sağlamak özellikle önemlidir. MG'de enerji üreten sistemlerin yanı sıra enerji tüketen sistemleri de kullanarak fosil yakıtların tüketiminden kaynaklanan kirlilik miktarını azaltma ve güç sisteminin güvenilirliğini sağlama hedeflenmektedir.

Bu tez, Rüzgar Türbini Üretim Sistemleri (WTGS), Elektrikli Araçlar (EV'ler), Fotovoltaik Üretim Sistemleri (PVGGS) ve Biyokütle gibi çeşitli DER'lerin dağıtım ağlarında aynı anda genel harcanan enerjiyi, termik santrallerden kaynaklanan hava kirliliğini ve toplam şebeke güç kaybını azaltmak için mümkün olan optimum tasarımı elde etmeyi hedeflemiştir. Bu planlanmış hedeflere ve faydalara ulaşmak için çok amaçlı optimizasyon ve hesaplama sistemi yapılandırılmıştır. Bu çalışmada, 24 saatlik bir süre boyunca değişen yük talebi altında enerji dağıtım sistemi üzerindeki etki analiz edilmiş ve bunun için farklı hesaplama modelleri kullanılmıştır. Ayrıca, dağıtık şebekenin yoğun olduğu/olmadığı saatlerde elektrikli otomobillerin deşarj/şarj modeli dikkate alınmıştır. Etkin kullanım imkanı sebebiyle, dağıtık enerji şebekesinin düzensiz ve sürekli olmayan optimizasyonunu için çok amaçlı karga arama algoritması kullanılmıştır.

Anahtar Kelimeler : Dağıtım Sistemi, Dağıtılmış Enerji Kaynakları, Emisyon, Karga Arama Algoritması, yük belirsizliği, Güç Kaybı, Gerilim sapması.

Bilim Kodu : 90544

ACKNOWLEDGMENT

First, I would like to express deepest gratitude to my supervisor Assoc. Prof. Dr. Muhammet Tahir Güneşer for his grateful motivation, guidance, support, continuous advice, and constructive suggestions toward the completion of this thesis. I would like to acknowledge my committee for their contributions in time and advice to improve this work. To my mother, I appreciate her for encouraging me to bring passion and love to whatever endeavor I undertake. She has been there since the beginning, supporting me throughout my degree programs, and even stayed with me to ensure the completion of this thesis, I am lucky to have such a wonderful family. I would like to thank my family and my wife for their support, encouragement, and patience throughout my studies. If I overlooked anyone, please accept my apologies, since there are so many nice and kind people, who provided me with moral support throughout this endeavor.

.

CONTENTS

Page

APPROVAL ii

ABSTRACT iv

ÖZET vi

ACKNOWLEDGMENT viii

CONTENTS ix

LIST OF FIGURES xii

LIST OF TABLES xiv

SYMBOLS AND ABBREVITIONS INDEX xv

CHAPTER 1 1

INTRODUCTION 1

1.1. HISTORY 1

1.2. NOVELTY OF THESIS 5

1.3. CONTRIBUTION OF THESIS 5

1.4. AIMS AND GOALS 6

1.5. SUBJECT, SCOPE 7

CHAPTER 2 8

LITERATURE REVIEW 8

2.1. WIND TURBINE 14

2.2. WIND POWER FUNDAMENTALS 15

2.3. MATHEMATICAL FORMULATION OF WIND TURBINE 16

2.4. MATHEMATICAL MODELLING OF PV 19

2.5. WIND TURBINE MODEL 21

2.6. DISTRIBUTED ENERGY 22

2.7. OBJECTIVES OF USING SCATTERED PRODUCTS 23

2.8. REASONS FOR THE APPROACH TO DISTRIBUTED GENERATION SOURCES 24

2.9. ECONOMIC BENEFITS OF DG FROM THE SUBSCRIBERS' POINT OF VIEW 25

Page

2.10. ECONOMIC BENEFITS OF DG FROM THE PERSPECTIVE OF AN ELECTRICAL DISTRIBUTION COMPANY 26
2.11. DISADVANTAGES OF USING SCATTERED PRODUCTS 27

CHAPTER 3 28
MATERIAL AND METHODS 28
3.1. MATHEMATICAL MODELLING 28
3.2. OPERATING CONSTRAINTS 31
3.2.1. Load flow evaluation 31
3.2.2. Voltage variation 32
3.2.3. Mathematical Model of PVGS 32
3.2.4. Mathematical Model of WTGS 35
3.2.5. Biomass power generation 39
3.2.6. Cost, power loss and emission optimization 41
3.3. REVIEW OF HONEY- BEE AND CROW SEARCH OPTIMIZATION ALGORITHM 41
3.3.1. Honey-bee algorithm 41
3.3.2. Crow Search algorithm 42
3.4. IMPLEMENTATION OF CSA ALGORITHM FOR SOLVING OPTIMAL DERS INTEGRATION PROBLEM 45

CHAPTER 4 49
EXPERIMENTAL RESULT 49
4.1. RADIAL DISTRIBUTION FEEDER 49
4.2. CASE 1 51
4.3. CASE 2 51
4.4. CASE 3 52
4.5. CASE 4 53

CHAPTER 5 69
CONCLUSION AND FUTURE WORKS 69
5.1. CONCLUSION 69
5.2. FUTURE WORKS 71

Page

REFERENCES 69

APPENDIX A CODES... 80

APPENDIX B 86

RESUME 89

LIST OF FIGURES

Page

Figure 1.1. Proposed layout for distribution management system. 6

Figure 3.1. PDF values and EOP of each hour at different solar irradiance level... 34

Figure 3.2. Output power of PV-module for each hour.. 35

Figure 3.3. PDF values and EOP of each hour at different wind speeds. 37

Figure 3.4. Hourly output power of WT Discharging /Charging Scheduling of EVs.. 37

Figure 3.5. The processing of the biomass (extraction and using). 39

Figure 3.6. Flowchart for the crow search algorithm. 44

Figure 4.1. Bus practical radial distribution feeder. 49

Figure 4.2. Uncertain load demand of each bus of the distribution network for 24 hours.. 50

Figure 4.3. (a) Hour wise generated output power by PVGS-1 for case 2, (b) Vehicles arriving for charging/discharging at each hour for case 2, (c) Hour wise generated output power by PVGS-1 and PVGS-2 for case 3, (d) Vehicles arriving for charging/discharging at each hour for case 3.53

Figure 4.4. (a) Hour wise generated output power by PVGS-1 and PVGS-2 for case 4, (b) Vehicles arriving for charging/discharging at each hour for case 4.. 54

Figure 4.5. Voltage profile of case 4 during 24-hours. 54

Figure 4.6. (a) Active power loss during 24 hours after DERs integration, (b) Reactive power loss during 24 hours after DERs integration, (c) Purchase active power cost from grid during 24 hours after DERs integration, (d) Voltage deviation during 24 hours after DERs integration. 58

Figure 4.7. 28- bus practical radial distribution feeder.. 59

Figure 4.8. Uncertain load demand of each bus of the distribution network during 24. Hoursz. 60

Figure 4.9. Best Cost vs. iteration. 60

Figure 4.10. Voltage profile vs. number of buses during 24-hours. 61

Figure 4.11. Real power loss (KW) vs. hours... 61

Figure 4.12. Reactive power loss (Kvar) vs. hours.. 62

Figure 4.13. Purchased Active Power Cost loss ($) vs. hours. 62

Figure 4.14. Voltage deviation (PU) vs. Hours... 63

Page

Figure 4.15. The results of all cases before and after DERs integration................... 64

Figure 4.16. Active power loss during 24 hours after DERs integration, Reactive power loss during 24 hours after DERs integration, Purchase active power cost from grid during 24 hours after DERs integration, Voltage deviation during 24 hours after DERs integration, a) Case 1, b) Case 2, c) Case 3, d) Case 4.. 66

LIST OF TABLES

Page

Table 3.1. Solar irradiance values in Tripoli 34

Table 3.2. Details of wind speed 36

Table 3.3. Parameter that used in the biomass power generation. 40

Table 4.1. Various cases for simulation analysis. 50

Table 4.2. Simulation results of all cases before and after DERs integration............ 55

Table 4.3. Optimal location and size of various DERs for different cases. 56

SYMBOLS AND ABBREVITIONS INDEX

SYMBOLS

CSA	: Crow Search Algorithm
RTP	: Regulated tariff plan
FC	: Fuel Cell
WT	: Wind Turbine
EVs	: Electric Vehicles
EU	: European Union
DERs	: Distributed Energy Resources
PVGS	: Photovoltaic Generation System
WTGS	: Wind Turbine Generation System
DG	: Distributed Generation
PSO	: Particle Swarm Optimization
NSGA II	: Non-Dominated Sorting Genetic Algorithm II
HAWT	: Horizontal Axis Wind Turbine
VAWT	: Vertical Axis Wind Turbine
PMSGs	: Permanent Magnetic Synchronous Generators
IEA	: International Energy Agency

CHAPTER 1

INTRODUCTION

1.1. HISTORY

Distributed generation basically consists of the production of electrical energy placing small energy sources as near as possible to points or areas of consumption (i.e., loads) [1]. In its most general sense, distributed generation may be defined as a connection with a power distribution grid or system installed at points nearest to where power will eventually be consumed [2]. The following are the general characteristics of distributed generation:

- System power losses decrease due to decreases in power flows in the system.
- Any energy output does not go back to the transport system.
- They generally operate at powers loads no greater than 3 kW and rarely exceed 10 kW of installed power.

Currently, industrialized countries generate most of their electricity in large, centralized facilities, such as fossil fuel plants (coal, natural gas) nuclear or hydroelectric. These plants are excellent at the scale of economic performance, but they transmit electricity normally over very great distances. However, power efficiency tends to be low and there is a greater and more deleterious environmental impact.

The placement of power plants tends to be dependent upon a number of factors, including those that are economic or environmental, as well as those relating to safety and logistics. These issues tend to be due in most part to the fact that a generated great distance exists between the points of power production and consumption. A striking example of this can be observed in how thermal power plants, because of their tendency to pollute the air, are purposely located far from urban centers and wherever and whenever possible as close as possible to sources of fossil fuel. Another prime example is the placement and location of hydroelectric plants on natural channels such as rivers.

Distributed generation gives another approach. It reduces the amount of energy lost in the electric power transmission network since electricity is generated very close to where it is consumed, sometimes even in the same building. This also reduces the size and number of power lines that must be built and maintained in optimal conditions.

Energy sources with a regulated tariff plan (RTP) have low maintenance, low pollution, and high efficiency. In the past, these features required operating engineers and complex plants to reduce pollution. However, modern embedded systems can provide these features with automated operations and non-polluting renewable energy, such as solar, wind and geothermal. This reduces the size of the plants improving the economic profitability.

Energy, which is a crucial component for expanding social government assistance, has basic significance in the supportable improvement of nations and generally, it characterizes the places of nations in the globalizing scene. Global warming, climate change and the accelerated global energy demands require optimal distribution of energy resources for uninterrupted, efficient, environment-friendly, and low-cost energy production by decreasing external dependence on resource procurement and finding sustainable environment-friendly resources. Until the middle of the 90s, the traditional energy distribution problem was largely about addressing limited resources under a single objective, such as cost minimization or profit maximization, while the diversity of resources considered in the last 20 years has increased and now, this problem has a structure that affects the optimal distribution of such resources. In [3], they adopted the objective programming approach to optimal distribution of 7 energy sources to fulfill their 12 objectives, including fulfilling the need for household lighting. Keeping in view objectives including emissions, cost, value creation for end users, and regional economic impact. In [4], they developed and presented an integrated resource planning model. Later, fuzzy dynamic programming approach was applied to deal with the resource allocation problem.

Distributed Energy sources i.e., Wind Turbine (WT), gas turbine, solar, Fuel Cell (FC), biomass, electric vehicles (EVs), micro turbine power etc. are gradually increasing globally as an electric power supplying system and these are located at customer region in distribution system. In latest years, distributed energy resources (DERs) became important as of their scientific, inexpensive, and ecological benefits. These characteristics cover wide variety of benefits i.e., evolvement of transmission line, decrease of greenhouse gases, sound pollution and decrease need on fossil fuels. By the end of 2025, the intention is to produce 25% of the overall power use of the European Union (EU) via DERs [5]. Moreover, EVs have frequently been optional as power source all over peak hours of the distributed energy system and useful for decreasing the oil utilization and air noxious waste emissions [6]. Since of good energy capability and ecological gain more than conventional vehicles that shows the future of EVs looks favorable [7].

In this thesis, for the setup of a DER in a distribution network, we used the multi objective crow search algorithm to solve multi-objective-based optimization tasks. Earlier, this optimization technique demonstrates successfully for various power system tasks such as transmission network expansion planning, economic load dispatch and unit commitment etc. This encourages the author to implement it for solving distribution system problem. In this study, a new multi-objective function design to identify the optimal locations along with optimum numbers of DERs in the distribution feeder under load uncertainty condition. This meta-heuristic approach motivates by the foraging nature of crow for finding the food source positions in the available search space. It is proficient, fast converging rate and effectual to handle composite non-linear constraint problems and having few controlling parameters. Due to these advantages, it selects as a preferred method to solve this problem. This problem having several objectives such as minimization of total real power loss, total cost and emission produced through thermal generators, improve voltage level, and reduce voltage deviation under load uncertainty.

Dispersed age entails producing electrical energy at a number of small power sources in locations as near as possible to where that generated power will be consumed. In general, distributed generation pertains to the idea of connecting a power distribution grid to points near to where consumption will occur. The basic features include:

- Recognition of the ideal positions and evaluations of a variety of DERs found in transportation systems utilizing a multi target crow inquiry streamlining strategy.
- A variety of cost valuations, including dynamic power consumption expenditure, the costs of setting up WTGS and PVGS as well as expenses related to O&M and the charging/releasing costs of EVs.
- It influences dynamic power consumption, actual and potential power loss, emissions age, and potential energy cuts after integration with the DERs.

In this thesis, mathematical DER models are employed in our analyses of the effects on distribution systems under unspecified daily demand for power. Moreover, we take into consideration the idea of peak and off-peak charging and discharging of Electrical Vehicles. By means of the multi objective crow search algorithm, which we use for its robustness, the non-continuous and non-bulgy optimization load is settled. Our results have been observed to be comparable with the Honey-Bee Colony and Particle Swarm Optimization methods. Micro grids are used to distribute power to a small number of consumers. Such power grids are located near to consumers, which has the advantage of lowering transmission line costs and power losses as well as an increase in the reliability of the system. Energy generation facilities in addition to the system upstream exist as distributed resources, such that a majority of the power is generally sourced from distributed generation facilities in addition to (whenever necessary) grids that are upstream. For the design and construction of molds, it becomes paramount to take into consideration matters of an economic and technical nature. A factor to consider when designing a grid is first to know the manner in which the cost and profitability of a grinder can be reduced.

1.2. NOVELTY OF THESIS

In this thesis, combined objective (multi-objective) crow search algorithm is employed for solving multi-objective-based optimization task, which is related to the DERs installation in distribution network. Earlier, this optimization technique has been demonstrated successfully for various power system tasks such as transmission network expansion planning, economic load dispatch and unit commitment etc. This gives confidence to author to execute it for resolving distribution scheme problem. In this manuscript, a new multi-objective function is designed to identify the optimal locations along with optimum quantities of DERs in the distribution feeder under load uncertainty condition. PVGS and WTGS mathematical model implement for computing the probability of wind speed and solar irradiance. So that, the expected output power can be evaluate. In addition, the charging/discharging concepts of EVs also consider in this work.

1.3. CONTRIBUTION OF THESIS

In this thesis for the optimization method, we used the metaheuristic method. This meta-heuristic approach is motivated by the foraging life of crow for finding the food source positions in the available search space. It is talented, fast converging speed and competent to handle complex nonlinear control functions and having fewer controlling parameters. Owing to these benefits, it has been chosen as a favored technique to solve this problem. This problem having more than a few objectives such as decreases of total cost, total real power loss and emission produced through thermal generators, improve voltage level, and reduce voltage deviation under load uncertainty.

The contribution in this thesis deals with the following matters:

- Impact on active power purchase, real and reactive power loss, emission generation and voltage deviation analyze after DERs inclusion.
- Various cost evaluates such as active power purchase cost, WTGS and PVGS installation cost and its O&M cost. In addition, charging/discharging cost of

EVs.

- Under load uncertainty condition, namely the identification of the best positions and ratings of a number of varieties of DER in a distribution network using a multi-objective crow search optimization technique.

1.4. AIMS AND GOALS

In this thesis an optimal integration of DER such as Photovoltaic Generation System (PVGS), Wind Turbine Generation System (WTGS), Electric Vehicles (EVs), and Biomass in supply network simultaneously will done for motive of abatement of overall power loss, overall cost and emanations dispatched through the thermal generators. To accomplish these planned purposes and profits, we will design a multi-objective function. The proposed layout for distribution management system is shown in following Figure 1.1.

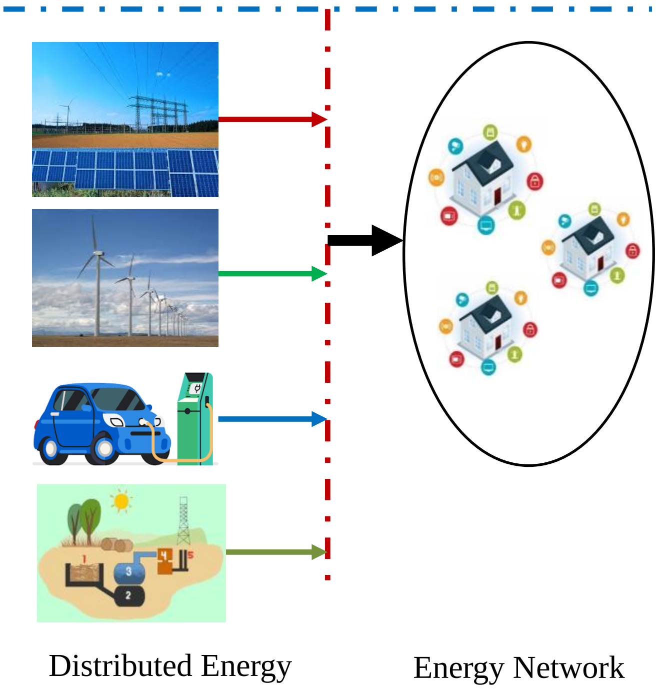

Figure 1.1. Proposed layout for distribution management system.

1.5. SUBJECT OF THESIS

In this thesis, a number of mathematical models of DER are used to analyze the effects on a distribution network under one day's worth of undefined power demand, including taking into account the charging and discharging of Electrical Vehicles during grid peak and off-peak periods. Taking a multi objective crow search algorithm approach due to its robustness, the non-continuous and non-bulgy optimization load becomes settled. The results are compared with other methods, such as the Honey-bee Colony Optimization methods. Micro grids are small networks that are created to provide a limited number of consumers. Sources of production are brought to consumers by these networks, which in turn lowers the costs related to transmission lines. This in turn enhances the reliability of the network. Most of the energy being produced generally comes from distributed generation sources and some (if necessary) upstream grids as the sources of energy for production are distributed sources. It is important to consider any economic and technical issues when designing and constructing molds. In the design of the grid, we need to know how to reduce costs with the profitability of a grinder necessarily being taken into account.

CHAPTER 2

LITERATURE REVIEW

Using renewable energy to generate power is a current research priority. Efforts to develop sources of different types of energy to expand the use of sustainable and renewable energy are increasing among all people of the world. The effects of fossil fuel depletion and environmental degradation are the most important reasons for the accelerating expansion of renewable energy in the 21st century [8]. Therefore, legislators and researchers pay a lot of attention to research in this field. For example, EU member states intend to use renewable resources and exploit at least 30% of its potential energy by 2030 [9]. There are several renewable energy sources, including biomass, wind, geothermal, solar, electricity, hydropower, and tidal energy in the renewable energies. Combined renewable energy sources can reduce harmful gas emissions and power consumption [10][11].

In last few years, many professionals, academicians, and researchers introduced and implemented a several heuristics and meta-heuristic approaches for deciding the positions and sizes of DERs in distribution feeders. In [12], presented an approach for evaluating the optimal size of hybrid WT/FC/Photovoltaic (PV) power systems using combined objective Honey Bee Colony method to reduce the purchase active real power cost, real power loss, emissions and maximize the stability in voltage profile. Multiple units of solar and wind generation have been incorporated in [13] by forming a combined objective function. This problem has been solved via combined objective Particle Swarm Optimization algorithm. Gampa and Das [14], formulated a combined objective function for determining the optimal allotments and ratings of different Distributed Generation (DG) systems of renewable energy resources in distribution feeder for decrease of voltage deviation, total power loss and total cost. Tan *et al.* [15], introduced a novel vaccine– enhanced artificial immune system algorithm for determining the optimal positions and sizes of biomass, wind and solar generation units. Along with this also recognized the optimal positions of tie-switches in distribution networks. Yang and Liao [16], developed A Fuzzy Mutation Adaptive PSO approach to resolve the multi-objective optimization problem by incorporating PV array for line loss minimization. Tolabi *et al.* [17], utilized a fuzzy ACO based approach to evaluate the optimal position and capacity of PV array along with the positions of tie-switches for the purpose of power loss reduction.

In the present work, combined objective (multi-Objective) crow search algorithm is employed for solving (multi-objective) based optimization task, which is related to the DERs installation in distribution network. This gives confidence to author to execute it for resolving distribution scheme problem. In this manuscript, a new multi-objective function is designed to identify the optimal locations along with optimum quantities of DERs in the distribution feeder under load uncertainty condition. It is talented, fast converging speed and competent to handle complex nonlinear control functions and having fewer controlling parameters. Owing to these benefits, it has been chosen as a favored technique to solve this problem. This problem having more than a few objectives such as decreases of total cost, total real power loss and emission produced through thermal generators, improve voltage level, and reduce voltage deviation under load uncertainty. For the improved details, the novel idea of the manuscript is a varying load command of each bus throughout 24 hours has been designed for industrial, commercial, and residential consumers to construct problem more practical.

Wen *et al.* [18] integrated the energy storage and wind generation units in distribution network through hybrid MOPSO algorithm for total expense minimization and voltage level enhancement. For PV-modules in a variety of distribution network time unstable load configurations minimizing reactive and active power losses and voltage divergences, Hung *et al.* [19] determined the ideal amount and location and optimum quantity with the formulation of a new combined objective Index function. a mathematical model of Battery Storage System (BSS) that offered a solution to issues, such as PVGS, of minimum line loss in distribution networks was put forth by Teng *et al.* [20] and in order to incorporate diverse types of power production from renewable energy sources in the distribution network, which in turn would reduce losses and improve voltages in the distribution process, a variation of the PSO algorithm was implemented in [21]. To lower losses in power and boost voltage levels, Khatod *et al.* [22], in their study, presented a meta-heuristic program that would find the best locations and sizes for PV-arrays and WTs in ring distribution systems. Atwa and El-Saadany [23] used a Mixed Integer Non-linear Programming method in the optimal assignment of wind based DGs to solve the problems found in deterministic distribution network planning. A methodology was presented by Atwa *et al.* [24][25], that would optimally integrate a number of types of renewable DGs to reduce yearly energy losses through MINLP.

According to [26], by determining the best locations of DG and EV charging stations in each zone of a distribution grid, a smart power control system can be created. Kayal and Chanda [27], in their study, used a PSO algorithm to determine and evaluate the best locations and ratings of renewable DGs to reduce losses of power even further. Niknam *et al.* [28][29], multi-objectively adapted the Honey Bee assistant optimization approach to integrate renewable energy sources, such as FC/WT/PV and distribution network reconfiguration to minimize deviations in voltage, loss of power, as well as to lessen the production of emissions and reduce overall costs. In a study conducted Rabiee and Mohseni-Bonab [30], the Non-Dominating Sorting Genetic Algorithm II (NSGA II), which determines the best levels of power for a number of distribution grids, was used with renewable energy sources. In the study by [31], the researchers created a hybrid algorithm through a combination of the ABC algorithm with Ant Colony Optimization (ACO) for a precise probabilistic DER installation. By doing so, the researchers managed to reduce simultaneously to a minimum the total power loss, voltage stability index, and emissions. Additionally, the overall network costs were simultaneously minimized in the combined objective framework.

Wind power generation, control, and integration have been the focus of research and development, and as a result, it is currently a very popular choice for generating electricity [34]. According to studies, wind power is typically regarded as the second most significant source of energy production [35]; as a result, work is still being done on harnessing its potential, grid integration, and PowerPoint tracking. Due to the fact that it has numerous uses, including recharging batteries and powering electric vehicles (EVs). The integration of a real-time EV charging controller and a battery charging controller is changing as researchers suggest and offer maximum power tracking techniques. Due to the high cost of wind turbines and the stochastic character of the wind as well as its various uncountable problems, researchers have not yet able to use the offered methods in all weather scenarios scenarios [36]. An emulator for a wind turbine is created to analyze the algorithms that have already been devised in order to solve this problem. The three functions of a wind turbine—parking, pitch angle modification, and recording the maximum power point—are all simulated by emulators [37]. The wind turbine emulator was created, and it was then evaluated in two different ways: model testing in real time and simulation.

The following initiatives are listed in the literature that already exists on wind turbine emulators: For the purpose of realizing the features of a wind turbine, a separately-excited DC motor was incorporated [38]. A digital signal processor was employed to create the proportionately Integral control logic of a wind turbine powered by excited DC motors simulator. According to studies [39], a commercial DC motor drive was used to simulate wind turbine characteristics. The reference model of the wind turbine, with a PI control, was implemented in this emulator using a dSPACE hardware board. A PI-controlled wind turbine emulator is presented in another work [40]. A straightforward gain-scheduled PI controller with some properties that matched those of a real-time wind turbine has been employed in study. In their investigation, they employed a DC motor to simulate wind turbine characteristics [41]. The output of the reference model is determined by the wind speed and the motor speed. The emulation control was implemented using a supervisory control and a personal computer. Emulation was almost 88% effective. A DC motor was controlled using armature voltage and field controls to record the necessary wind turbine characteristics in another work [42]. A PI control method was put into practice as a proportional control measure for controlling field flux using armature voltage management. A reference model for a wind turbine uses the motor speed and wind speed to generate the reference command. 90% emulation efficiency was reported by the researchers.

When the researchers used a DC motor that was individually energized, they were able to simulate real-time wind turbine characteristics [43]. An analog circuit approach was applied for the wind turbine's mathematical modeling. The wind turbine emulator's PI control was improved through restricted optimization, and it was achieved when the researchers employed a DC motor that was activated individually [44]. A wind turbine reference model produced the reference command based on a variety of factors, including pitch angle, motor speed, and wind velocity. A PI control is used to manage the torque that a motor produces. In this instance, the researcher reported an emulation efficiency of 91%. A PI-controlled DC motor can resemble a wind turbine in several ways, according to another study [45]. Wind speed, pitch angle, and motor speed were used to generate the reference torque in a wind turbine. The researchers implemented PI control using a DS 1104 hardware control board and a wind turbine reference model.

In a different study [46], open-loop DC motor control was examined in order to simulate the real-time characteristics of wind turbines. To do this, open-loop armature voltage control and field flux control from a wind turbine were used. Power resistors were used to manage the DC motor voltage, which increased power losses and reduced system efficiency as a whole. In a research paper [47], the authors used MATLAB to simulate a wind turbine that used a DC motor and its associated control. The required current signal was produced by the reference wind turbine model depends on wind speed, pitch angle, and DC motor speed. A PI control has been utilized to regulate the torque of the DC motor and simulate the characteristics of a wind turbine. The researchers previously reported an emulator for a proportional derivative-controlled wind turbine with fuzzy logic in a research publication [48]. We employed fuzzy logic control to regulate the torque and speed of a DC motor. With fuzzy logic control, the system's emulation efficiency was over 92%, as demonstrated by a comparison between a traditional PI control and a fuzzy logic controller. a wind turbine powered by a permanent magnet DC motor simulator was employed in a different investigation [49]. They looked at a wind turbine's hardware implementation and simulation. With the help of a four-quadrant DC motor controlled by a chopper, they proposed a PI torque-control method and imitated several wind turbine characteristics [50]. They implemented the wind turbine emulation control using Lab View software and a hardware control board for a microcontroller. The researchers-built speed and current controls using the PI control method. Emulation effectiveness of the system was close to 91%. Open-loop FPGA control DC motor research [51] reveals that the model approximated some aspects of wind turbines. They employed a wind velocity-based PWM pulse for a motor fed by a DC–DC converter. Program for a reference model of a wind turbine was an FPGA control board. Additionally, a wind turbine emulator for standalone applications was created [52].

Pollution-fighting capabilities of wind, solar, and other renewable resources are enhanced by advanced wind-based power generation technology, such as kinetic energy is captured by wind turbines of the wind to produce electricity. Since no greenhouse gas is released and wind power is a feasible substitute for harmful fossil fuels, there is a noticeable difference in how the environment is affected. In comparison to other renewable energy sources, the cost of producing wind power has decreased as a result of various breakthroughs; nonetheless, research on wind turbines should keep improving it to become an even more competitive energy source [53, 54].

Too many different types of variable speed generators are used in wind turbines. Numerous research have suggested that Permanent Magnetic Synchronous Generators (PMSGs) offer some advantages over other types of generators. PMSGs operate at modest rotational speeds and without a gearbox. The advantages of PMSGs include their high efficiency and minimal maintenance requirements [55-58].

Although a wind turbine is often equipped with fixed frequency induction generators, not all wind conditions will result in increased power output. The performance of wind power generation systems needs to be continually improved; however the inverter unit's efficiency needs work. To increase and improve efficiency and dependability, a new controller is implemented. This controller consists of a back-to-back space vector and MPPT that will be merged into PWM. Additionally, We'll measure the rotor speed and compare it to the ideal rotor speed. Both the inverter and the pitch angle controller saw improvements as a result of the performance regulation. Various characteristics, including the aerodynamic turbine torque, have been altered by combining wind speed [59-62].

2.1. WIND TURBINE

While the control system maintains the output, the electric generator's shaft rotates and produces electricity. There are two different types of wind turbine designs that can be categorized according to how they rotate: Wind turbines with a horizontal axis and a vertical axis (VAWT). In honor of its creator, Darrieus, the latter turbine is occasionally referred to as a rotor [32]. The majority of the wind energy is captured by HAWTs throughout the day, and their blades are changed during windstorms. The pace at which the wind turbines operate might be either variable or constant. When a constant-speed turbine is employed, the rotor's angular speed stays constant regardless of changes in the wind. One benefit of this mode is that it does not need pricey power electronics, such as converters and inverters. The rotor speed is limited, which prevents a turbine from operating at maximum efficiency in strong winds. As a result, compared to turbines with variable wind speeds and a set rotor speed, a constant-speed turbine produces less energy when the wind speed is low. Even when the wind speed is less than the rated wind speed, the wind speed and rotor speed are proportional [33]. Numerous elements, such as rotor blade tilt, turbine speed, turbine size and shape, rotor geometry (regardless of whether the turbine is a HAWT or VAWT type), wind speed, and turbine area, affect the output power and torque of a wind turbine. There is a relationship between various variables and the output power that contributes to the mathematical model of the wind turbine. This mathematical model of the wind turbine must be developed in order to understand the behaviors of the wind turbine in its operational region and, in addition, to control the operational performance of the wind turbine. This thesis proposes a particular design of wind turbine that achieves the goals.

We have outlined the methodology for this thesis in this part.

2.2. WIND POWER FUNDAMENTALS

Multiple studies have shown that the synchronous generator in the model of the full wind power generation system increases system performance, as do the generator-side and grid-side control strategies. Pitch angle control models, PMSG wind turbine models, generator-side inverter models, and grid-side inverter models are included in this sort of control mechanism and model system.

It is clear from numerous research on the wind turbine system that the system's efficiency is increased by the inclusion of some controls for a real permanent magnet synchronous generator as well as grid-side and generator-side controls. Control of the pitch angle, grid-side inverter, PMSG wind turbine, and generator-side inverter models are included in the control methods and the system in question. By providing the varying the grid-side and generator-side inverter controllers use pulse width modulation to offer Maximum PowerPoint Tracking (MPPT) and decouple current to the x and y axes of their inverters. some reactive power controls from active power controls. The researchers employed a conventional PI controller in order to enhance the control method. They combined an inverter for both the grid and the generator side as well as a pitch angle controller. They used MATLAB Simulink to simulate and validate the performance. Results (where autonomous controllers are utilized) would clarify the effects of the integrated PMSG wind turbine [63, 12, 14].

In [64], the author has used linear programming to reduce the cost of creating and operating gratings and how to provide optimal energy supply by each producer.
In [65], the author has been discussing how to provide the load by several producers and obtaining the optimal answer by combining the linear method and the genetic algorithm.

Nonlinear programming has been used in [66] to reduce the cost of grinding, along with the reduction of pollutants. Reliability is another factor that contributes to the decision-making process.

In [67] and [68], the author examines the effect of micro grid on increasing reliability in the network, and suggests that reliability will increase with decreasing interruptions and time to fix it.

2.3. MATHEMATICAL FORMULATION OF WIND TURBINE

When a force F is applied while doing work W to move the object from its stationary position to a distance s, the object's kinetic energy (E), which is given as E = W = Fs, has a velocity of v and a mass of m. According to Newton's second law of motion:

$$F = ma \tag{2.1}$$

The kinetic energy will be:

$$F = mas \tag{2.2}$$

Solid motion kinematics are shown by $V^2 \equiv u^2 + 2as$ whereas u is the starting speed of the object. It stands for $V^2 \equiv u^2 + 2as$. $a = \frac{V^2}{2s}$ since we're assuming that the object's initial velocity is zero. Equation 2.2 gives us:

$$E = \frac{1}{2}mV^2 \tag{2.3}$$

The basis for this kinetic energy formulation is the fact that, even if the mass of every solid object remains constant, the mass of wind (moving air) is not because it is a solid since its velocity and density are changeable and it is not a solid because it is a gas. This is presuming that changes in temperature or altitude do not significantly affect the air density. The kinetic energy rule is depicted in equation 2.3 [69]. Equation 2.3 can be used to calculate the mass m and velocity V w (wind speed) of the kinetic energy (joules) of air. The rate of change in kinetic energy is represented by wind power P, so:

$$p = \frac{dE}{dt} \equiv \frac{1}{2}\frac{dm}{dt}v_W^2 \tag{2.4}$$

Here, $\frac{dm}{dt}\,\rho AV_w$ displays the mass flow rate $\frac{dm}{dt}$, A denotes the area of the wind flow, and denotes the air density. Equation 2.4 is the following using this knowledge:

$$P = \frac{1}{2}\rho A v_W^3 \tag{2.5}$$

Upstream-downstream wind power is measured in watts and is known as mechanical power Pw. differential [70], is extracted by the rotor blades and is given below:

$$P_w = \frac{1}{2}\rho A v_w (v_u^2 - v_d^2) \tag{2.6}$$

In this equation, v_u indicates the v a represents the upstream wind speed (m/s) at the rotor blade entrance point, and v_d indicates the downstream wind speed (m/s) at the rotor blade's exit point. We will demonstrate in the next sections of this thesis that these velocities combine to produce a particular speed ratio on the blade-tip. The following equation was created using the mass flow rate:

$$\rho A v_w = \frac{\rho A(v_u + v_d)}{2} \tag{2.7}$$

Here, v_w is the mean speed of the turbine rotor blades during entry and exit. This expression yields Eq. 2.6 will be $P_w = \frac{1}{2}\rho A v_w (v_u^2 - v_d^2)(\frac{v_u + v_d}{2})$ and that can be simplified as given below:

Here, the turbine rotor blades' entry and exit velocities are averaged to form the value v_w. Equation 2.6 will be $P_w = \frac{1}{2}\rho A v_w (v_u^2 - v_d^2)(\frac{v_u + v_d}{2})$ using this expression, and it can be reduced as follows:

$$P = \frac{1}{2}\rho A v_u^3 C_P \tag{2.8}$$

The C_P expression, which is a component of the upstream wind power consumed by the rotor blades, is given in Equation 2.8. Because it was first proposed in 1919 by German scientist Albert Betz, C_P is also known as the Betz limit. It is also known as rotor efficiency and the rotor's power coefficient, and it fluctuates with changes in the wind turbine's tip speed ratio rather than remaining constant. The downstream-upstream wind speed ratio is shown here by the symbol $\boldsymbol{\lambda}$:

$$\lambda = \frac{v_d}{v_u} \tag{2.9}$$

Or

$$\lambda = \frac{blade\ tip\ speed}{wind\ speed} \tag{2.10}$$

The wind turbine tip speed ratio is shown by the symbol λ*.* The rotating speed of the turbine and the length of the blades can be used to calculate the per second blade tip speed:

$$blade\ tip\ speed = \frac{angular\ speed\ of\ turbine(\omega) \times R}{wind\ speed} \tag{2.11}$$

The turbine radius is denoted by R in this equation, and is expressed in radian per second ω.

Other elements in a whole system that prevent full energy conversion include bearings, the gearbox, the number of blades, and the geometry of the blades. Only 10–30% of wind energy is converted into useful energy. The air density is shown here with a different flow input quantity ρ. And stands for the relationship between air pressure and temperature. In this case, a rise in raises air pressure while lowering air temperature. According to the state's equation, it is as follows:

$$P = \rho RT \tag{2.12}$$

In this equation R stands for the gas constant. Elevation causes a drop in pressure and temperature. This demonstrates the significance of the site's location since, as was already established, elevation has a significant impact on power generation because the air density varies.

2.4. PV MODELLING

A current source that functions in parallel with a diode in an analogous circuit is a PV cell. A actual equivalent circuit model includes more series and parallel resistors when it is employed. It should be remembered that a PV cell functions like a p-n junction diode and cannot generate electricity when there is no sunshine. The amount of sunlight that hits a PV cell will determine the actual current that comes from it (Photocurrent).

This section has provided the mathematical model of the PV cell. A decrease in voltage at the p-n junction determines how much power the PV cell will produce (diode).

$$V = \left(\frac{NKT}{Q}\right) ln \frac{I_L - I_o}{I_o} + 1 \qquad (2.13)$$

In this case:

The light-generated current (Ip h (A)) is displayed in IL.
N represents the diode ideality constant.
The open circuit voltage is denoted by V.
K stands for the Boltzmann constant (1.381x 10-23JK-1)
The saturation diode current is referred to as Io (A)
Temperature is T. (Kelvin)
Q displays an electron charge (1.602 x 10-19 Coulombs)

current produced by light:

$$I_L = \left(\frac{G}{G_{ref}}\right) * (I_{L\,ref} + \propto_{Isc} \left(T_C - T_{C\,ref}\right)) \qquad (2.14)$$

Here

G ref denotes radiation of 1000 W/m2 under ideal circumstances.

G is the radiation unit (W/m2).

Tc denotes the temperature as it is right now.

The photoelectric reference current, or IL ref, operates at 0.15A under typical conditions.

Light generated current/radiation is referred to as IL.

When A/K = 0.0065AK-1, αISC stands for the short circuit current's temperature coefficient.

The module temperature displayed by TC ref is 298.0 K under ideal conditions.

The following is the reverse saturation current:

$$Io = I_{or}\left(\frac{T_c}{T_{ref}}\right)^3 \; e^{\frac{(Q*Eg)}{(K*N)*\left[\left(\frac{1}{Tcref}\right)-\left(\frac{1}{Tc}\right)\right]}} \quad (2.15)$$

$$I_{or} \;\; = \frac{I_{scn}}{e^{\left(\frac{V_{ocn}}{N*V_{tn}}\right)}} \quad (2.16)$$

In this instance

The saturation current is indicated by I_{or}.
The reverse saturated current is represented by Io.
Ish = IL, or short circuit current
EG is short for silicon band gap (1.10 eV)
N displays the optimality factor (1.50)
The most current is produced by the cell and is created when there is a short circuit: Volts = 0.00V.

$$I_{sh} = (I_L - I_o) * \left(e^{\frac{eV}{KT}} - 1\right) A \quad (2.17)$$

2.5. MODELLING OF WIND TURBINE

Peak output from wind turbines is predicted to occur at wind speeds of 15 m/s. Cut-in wind speed (nearly 5 m/s) is related to the starting wind turbine speed. The generator's greatest power output was delivered when the rated wind speed was between 10 and 17 m/s. The phrase "cutout wind speed" refers to the range of wind speeds between 17 and 30 m/s that put the rotor at danger of damage. Power control techniques for the wind turbine include pitch control and stall control.

The formula in Equation 2.18 is useful for calculating wind power. output.

$$P_w = 0.5\rho C_p A v_\omega^3 \quad (2.18)$$

Where stands for air density, P_w for wind energy captured, v_ for wind speed, Cp for power coefficient, and R for rotor blade radius. Expressions 2.19, 2.20, and 2.21 describe the relationship between a power factor and the pitch angle of a blade.

$$C_p(\lambda, \beta) = C_1(\frac{C_2}{\lambda_i} - C_3\beta - C_4)e^{\frac{-C_5}{\lambda_i}} + c_6\lambda \quad (2.19)$$

$$\lambda = \frac{\omega_t R}{v} \quad (2.20)$$

$$\frac{1}{\lambda_i} = \frac{1}{\lambda + 0.08\beta} - \frac{0.35}{\beta^3 + 1`} \quad (2.21)$$

The turbine speed It is expressed in this equation as radians per second, ω_r. The optimal power coefficient value is 0.48 when equals 0^0, the tip speed ratio is 8.10, and the power coefficient reaches its maximum value. The maximum C_p's Betz limit is 59.3%.

The following is how mechanical torque is obtained:

$$T_m = \frac{P_m}{\omega_r} \tag{2.22}$$

The torque equation can be expressed as Equation 2.23 when the drive train is modeled as a single rotating mass.

$$J\frac{d\omega}{dt} = T_m - T_{em} - K.\omega \tag{2.23}$$

Here, T_{em},K, and J stand for the respective values of viscous friction, electrical torque, and the total inertia constant.

Equation 2.24's representation of the torque created in terms of electrical characteristics reads as follows:

$$T_e = \frac{3}{2}\frac{P}{2}\left(i_{qs}i_{dr} - i_{ds}i_{qr}\right) \tag{2.24}$$

2.6. DISTRIBUTED ENERGY

Distributed generation is the generation of electricity from small energy sources. Distributed generation refers to cases where electricity is generated at or near the point of consumption. Scattered generation are small-scale power plants with a maximum production capacity of 25 MW. Scattered production was since current and voltage drops were observed in some places. This plan was proposed to fill these gaps. Distributed generation is divided into two categories: simultaneous generation of electricity and heat, as well as electricity, cold and heat, which stands for Combined Cooling Heat and Power. Simultaneous generation means generating electricity along with other forms of energy and using all items simultaneously. A co-generator is a generator whose heat dissipation is used directly or recycled to produce hot water, steam, or other applications. An important advantage of cogeneration is that its effective electrical efficiency is more than 1.5 times that of thermal power plants [71]. Currently, most industrialized countries generate their electricity in large, concentrated facilities such as fossil fuels (coal, gas), nuclear or hydropower. These plants reduce costs well, but they usually carry electricity over long distances and affect the environment. Scattered production is another method. This method reduces the amount of energy lost in the transmitted electricity because electricity is generated very close to where it is consumed, or even in the same building. This reduces the size and number of power lines to be built.

Although distributed generation is a new concept in the economic literature of the electricity industry, its true nature is not new. In the early days of power generation, distributed generation was a pervasive principle, with the first power plants feeding only their immediate and neighboring subscribers. Since direct current networks were the first power grids, on-site storage resources such as batteries were used to balance production and consumption. Later, with the advancement of technology (such as the emergence of AC networks), it became possible to transmit electricity over long distances [72].

Gradually, massive electrical systems, including power plants and large transmission and distribution networks, emerged. The balance between production and consumption was achieved through the average effect of many instantaneous loads, and the security of these large networks was increased so that in the event of an error and out of orbit of one source, other resources in the network were responsible for compensating production.

In recent decades, technological advances, economic changes, and environmental regulations have led to a great deal of interest in the concept of distributed production. The International Energy Agency (IEA) announced in 2002 that these five key factors have contributed to the pervasiveness of the concept of distributed generation: the development of distributed generation technologies, restrictions on transmission lines, increasing sustainable energy demand by subscribers, privatization of electricity markets and climate change concerns.

2.7. OBJECTIVES OF USING SCATTERED PRODUCTS

The goals of using distributed products are different from the distribution company's point of view and from the common point of view. In fact, if the distribution company's owner's DG, the goals could be to liberalize the distribution network capacity, improve system reliability, generate electricity and heat at the same time, improve power quality and voltage profiles, and reduce losses. If the ownership of the DG is jointly owned, these goals could be the sale of electricity and participation in the energy market, the sale of electricity as an ancillary service, the improvement of its reliability, or the incentives received from the distribution company, and so on. Unfortunately, because most of the dispersed products are owned by the subscribers, the distribution companies have less control over the size and location of the dispersed products. Consequently, to save you the terrible effect of dispensed merchandise on various machine parameters, there ought to be a well-known and comprehensive well-known for control, set up and location of these merchandise. In preferred, the reason of using disbursed technology sources in distribution networks is to provide all or part of the community energy intake complete-time or part-time, amongst which the principal cause is to generate lively strength.

2.8. REASONS FOR THE APPROACH TO DISTRIBUTED GENERATION SOURCES

Inside the old structure of the electricity enterprise in advanced international locations and the present-day situation of many countries, the duties of electricity technology, transmission and distribution have been the obligation of included electricity businesses. The growth in strength calls for in current years in many countries has averted those companies from responding efficaciously to this excessive call for. because of blackouts, electricity outages and gadget disasters, took place in many countries, especially America, and consequently fees rose sharply during top intervals. on the same time, at the side of the financial growth of countries, which led to a boom in the amount of energy they wished, the difficulty of power satisfactory and reliability also have become essential.

In addition, the oil crisis in 1995 prompted many countries that were dependent on fossil fuels in their industry to find suitable alternatives to these fuels. It also became more important to find a suitable alternative to fossil fuels as public awareness of environmental issues increased. Studies show that renewable energy sources, including solar, wind, water, biomass, geothermal and energy, which are environmentally friendly, can be a good alternative to fossil fuels. Thus, factors such as the restructuring of the electricity industry, the need to increase system capacity and the advancement of technologies simultaneously, are the basis for the introduction of distributed generation technologies [73].

The frequency of many factors has increased the tendency to use distributed generation systems, which in general can be divided into five groups as follows:

- Significant industrial advances in the manufacture and application of related technologies
- Restrictions on the construction of transmission lines
- Enter the discussion of the electricity market and related issues in the power system
- Increased customer demand for high-reliability service
- High sensitivity to environmental pollution

2.9. ECONOMIC BENEFITS OF DG FROM THE SUBSCRIBERS' POINT OF VIEW

- Reducing energy purchase costs, especially in the case of thermal loads (steam, hot water, and cooling system); In CHP method, steam or hot water required for various processes can be provided or used in cases where the environment needs to be heated or cooled.
- Reducing worries caused by energy rate fluctuations: DG allows subscribers to take more risks in the energy market, because in fact, subscribers have freed themselves from these fluctuations by using DG.
- Increased reliability: DG can reduce network outages, which in turn reduces downtime and reduces safety concerns.
- Improving power quality: DG can deliver high quality power and energy to subscribers and therefore this reduces or eliminates the existing concerns in the field of mains voltage fluctuations and harmonics that affect the sensitive loads of subscribers. Lays.

- New source of revenue: DG allows subscribers to sell their generated energy or have a marketing aid.

2.10. ECONOMIC BENEFITS OF DG FROM THE PERSPECTIVE OF AN ELECTRICAL DISTRIBUTION COMPANY

- Preventing the increase of network capacity: DG provides energy as an auxiliary and additional source and therefore can to some extent prevent the distribution company from creating a new system of production, transmission and distribution [74].
- Reduction of electrical losses in the transmission and distribution sector: With the installation of DG, the transmission and distribution network to transport and provide energy to subscribers becomes smaller and therefore losses are also reduced.
- Delaying and updating the transmission and distribution networks: Using DG, distribution companies can respond to the growth of cargo and therefore improve the capacity with a time delay.
- Reactive power supply: Some DG technologies such as reciprocating engines can produce reactive power. This helps to strengthen and stabilize the mains voltage.
- Reducing demand density and energy transfer: By installing a power generation system at or near the point of consumption, the effective length of the transmission and distribution network increases and the network capacity is released to respond to other subscribers.
- Peak hour: DG can reduce the demand of subscribers during peak hours, which will reduce costs.
- Reducing the reservation margin: with the installation of DG, the total demand of the network decreases and the production capacity improves, and therefore there is a need for less reservation in the network.
- Improving power quality: By installing DG, the negative effects of power quality such as voltage and unfavorable frequency in the network are reduced.

- Increasing power capability: Using DG can reduce or eliminate blackouts in certain parts of the distribution network.

2.11. DISADVANTAGES OF USING SCATTERED PRODUCTS

Despite all the benefits of DG, we need to pay special attention to its potential negative effects on the distribution network, perhaps most of which are voltage level issues and protection coordination. It also complicates the network and thus the development of the network protection system, as well as the operation and control of the network. Connecting DGs to the grid creates a harmonic in the grid and reduces the short circuit impedance. Also, if the DG connected to the network works as an island during a blackout, it can be dangerous for network repairmen [75].

CHAPTER 3

MATERIAL AND METHODS

3.1. MATHEMATICAL MODELLING

From the environmental concerns and varying load calls in relation to the system, the focus of our attention has been on the execution of diverse DERs in distribution machine. consequently, a multi-objective health characteristic has been created for figuring out the most excellent positions and ratings of DERs. With regard to complete work and real power loss, set up price and emission sent via the grid. This stochastic multi-goal optimization task is formulated as seen on Eq. (3.1).

$$Minimization\ MOF = w1 \times \underbrace{\left(C_p + PV_{instt} + PV_{O\&M} + W_{instt} + W_{O\&M} + Bio_{instt} + Bio_{O\&M} + \sum_{t=1}^{24} C_{EV}(t)\right)}_{Total\ Cost} + w2 \times \underbrace{\sum_{t=1}^{24} P_{TLoss}(t)}_{Power\ Loss} + w3 \times \underbrace{\sum_{t=1}^{24} E_{EMSN}(t)}_{Emission} \tag{3.1}$$

Fifth term of the fitness function shows the installation cost of Biomass (Bio_{instt}) and it is evaluated using (3.2). Fifth term is Biomass O&M cost, it is evaluated using (3.3).

$$Bio_{instt} = P_{Bio} \times CP_{Bio} \tag{3.2}$$

$$Bio_{O\&M} = \sum_{y=1}^{yr} PW^{y} \times 0.03 \times Bio_{instt} \tag{3.3}$$

Here, CP_{Bio} and P_{Bio} is the capital cost of biomass installation and output power of biomass respectively.

The total cost portion is multiplied by lower value of weighting factor ($w1$), power loss and total emissions are multiplied by the higher value of weighting factor ($w2$) and ($w3$) respectively. The main reason behind for multiplying weighting factors is to linearize each term of the fitness function adequately to find optimal outcomes.

W1, w2 and w3 are coefficient for multi objective optimization. W1=w2=w3= 0.5 where C_p is the primary term of the goal function of the acquired real power cost from the grid defined using Eq.(3.4) as a linear function [76]**:**

$$C_p = \sum_{y=1}^{yr} PW^y \times 365 \times \sum_{t=1}^{24} \rho_E(t) \times P_{real}(t) \tag{3.4}$$

Here, PW is the present worth, which is defined as $\frac{(1+infR)}{(1+intR)}$. The variable yr is the number of years, ($In\ tr$) and ($in\ f\ r$) are, respectively, the interest rate (12.5%) and inflation rate (9%). $Preal(t)$ he purchase active power via the grid, ρE the spot electrical energy market cost confirmed a day previously. The cost of setting up the PVGS ($PVinstt$) is denoted by the term that follows the goal function by being manipulated using Eq.(3.4). O&M of PVGS ($PVO\&M$) cost, the third term, is evaluated [77][78] using Eq. (3.5).

$$PV_{instt} = PV_{out} \times CP_{PV} \tag{3.4}$$

$$PV_{O\&M} = \sum_{y=1}^{yr} PW^y \times 0.03 \times PV_{instt} \tag{3.5}$$

where $CPPV$ and $PVout$ are the PV installation resource cost and PVGS output power, respectively. WTGS ($Winstt$) is calculated using Eq. (3.6) and the WTGS O&M cost [77][78] using Eq. (3.7).

$$W_{instt} P_w \times CP_w \tag{3.6}$$

$$W_{O\&M} = \sum_{y=1}^{yr} PW^y \times 0.01 \times W_{instt} \tag{3.7}$$

where CP_W and P_W are the WT installation capital cost and WT output power, respectively, C_{EV} the EV charging/discharging cost () from or to the grid [79][80]. Vehicle vendors are able to select optimal discharging/charging programs for their vehicles, which can be computed according to Eq. (3.8).

$$C_{EV}(t) = \rho_E(t)[\eta_{dch}P_{dch}(t) - \eta_{ch}P_{ch}(t)] \tag{3.8}$$

where η_{ch} / η_{dch} are respectively the charging/discharging efficiencies of EVs, and $P_{ch}(t)$ / P_{dch} (t) are respectively the charging/discharging power of the gradable vehicle. The sum of the active power loss (P_{TLoss}) occurs over a 24-hour period over every branch of the distribution system is the seventh term of the fitness function, which is calculated as in Eq. (3.9):

$$P_{TLoss} = \sum_{\substack{i=1 \\ i \neq j}}^{j} P_{Loss}(i, j) \tag{3.9}$$

The last term in the goal function is the quantity of emissions occurring in a 24-hour period through the grid. These emissions consist of nitrogen oxide (NO_x), carbon dioxide (CO_2) and sulphur dioxide (SO_2) [31], the total quantity of which over a 24-hour period can be calculated using Eq. (3.10):

$$E_{EMSN} = \sum_{t=1}^{24} P_{real}(t) \times (CO_2 + NO_X + SO_2) \tag{3.10}$$

In equation (3.10), every term is normalized through weighting aspect technique. The value element in Eq.1 is very higher due to the fact it's far associated with the value of buy active electricity, PVGS set up, PVGS O&M, WTGS set up, WTGS O&M, and EVs charging/discharging even as energy loss and emission produced thru grid are pretty decrease. as a result, the whole value portion is elevated via decrease fee of weighting aspect (w1), energy loss and overall emissions are increased by means of the better fee of weighting thing (w2) and (w3) respectively. the primary motive at the back of for multiplying weighting factors is to linearize every term of the health function appropriately to locate premiere results.

3.2. OPERATING CONSTRAINTS

In this investigation, these DERs play a crucial function in electricity networks by using operation and technology. these act as DGs by way of distribution community. those EVs which might be competent for inclusive of electric strength into the grid are described as grid related vehicles. all through peak hours, EVs transfer electric energy to the device to satisfy the height demand requirement and off-top intervals of the machine these automobiles may be rate up to specific most limit and because of EVs decreases the emission charge which is generated from thermal strength plant and complements the reliability of the network.

in this observe three diverse DER aggregators had been considered to apprise by the Distribution control system (DMS). DMS is transmitting electric electricity as per info collected from those aggregators. WTGS aggregator will combination wind power generation information via WTGS. within the similar manner, PVGS aggregator will accumulate statistics concerning solar strength manufacturing through PVGS. In case of EVs, anyone vehicles proprietor in most cases registered their man or woman car to EVs aggregator for discharging and charging motive. Then, EVs aggregator will send data to the automobile's proprietor either for discharging and charging in line with the load settings of the grid. This painting has implicit the smart distribution device which can provide surety for operation and accurate use of these DERs with the recent infrastructure and clever calculation techniques. The numerical models of these DERs are as discussed under.

3.2.1. Load flow evaluation

Accumulation of power procured through the grid, PVGS, WTGS and EVs must fulfill the load demand. It is expressed using as seen on Eq (3.11),

$$\sum_{t=1}^{24} P_{real}(t) + \sum_{t=1}^{24} P_{WTGS}(t) + \sum_{t=1}^{24} P_{PVGS}(t) + \sum_{t=1}^{24} P_{dch}(t) = \sum_{t=1}^{24} P_{ch}(t) + \sum_{t=1}^{24} P_{Load}(t) + \sum_{t=1}^{24} P_{TLoss}(t) \quad (3.11)$$

The voltage value is between minimum voltage and maximum voltage. It can be shown as equation (3.12).

$$V_i^{min_i{}_i^{max}} \tag{3.12}$$

For the current, it should be less than the threshold value. It can be shown as equation (3.13).

$$I_{ij} \leq I_{Th}^{rated} \tag{3.13}$$

The electric vehicles energy should be limited as the number of the electrical vehicle that shown in equation (3.14).

$$\sum_{t=1}^{24} EV(t) \leq N_{EV} \tag{3.14}$$

Bus number one is considered as a slack bus and voltage value of this bus is 1 pu.

3.2.2. Voltage Deviation

Bus voltage is one of the most vital indications to examine the power excellence. If the large disturbance happens in the voltage amplitude, this indicates the indigent behavior of the system. The overall total voltage deviation during 24 hour of each bus is evaluated using (3.15).

$$V_{deviation} = \sum_{t=1}^{24} \sum_{i=1}^{NB} \frac{|V_{rated} - V_i|}{V_{rated}} \tag{3.15}$$

3.2.3. Mathematical Model of PVGS

The production power generation via PV module principally depends upon the concentration of solar irradiance. The hourly irradiance incident at a fixed place mostly they assume a binomial allocation, it is an array of two linear unit-modal distribution functions [19][20]. A beta Probability Density Function (PDF) is developed to both unit-modals, as set out in the following:

$$f_b(s) = \begin{cases} \frac{\Gamma(\alpha+\beta)}{\Gamma(\alpha)+\Gamma(\beta)} \times s^{(\alpha-1)}(1-s)^{(\beta-1)} & for\ 0 \le s \le 1,\ \alpha \ge 0,\ \beta \ge 0 \\ 0 & otherwise \end{cases} \quad (3.16)$$

Here, s stands for the solar irradiance (kW/m^2). α and β are the beta distribution function *fb(s)* parameters, these can be calculated using (3.17) and (3.18).

$$\beta = (1-\mu_s) \times \left(\frac{\mu_s \times (1+\mu_s)}{\sigma_s^2} - 1\right) \quad (3.17)$$

$$\alpha = \frac{\mu_s \times \beta}{1-\mu_s} \quad (3.18)$$

The photovoltaic output power can be written as (3.19) [20].

$$PV_{out}(s) = N \times F_F \times V_y \times I_y \quad (3.19)$$

$$V_y = V_{oc} - V_k \times T_{cy} \quad (3.20)$$

$$I_y = s[I_{sc} + I_k(T_{cy} - 25)] \quad (3.21)$$

$$F_F = \frac{V_{MPT} \times I_{MPT}}{V_{oc} \times I_{sc}} \quad (3.22)$$

$$T_{cy} = T_A + s\left(\frac{N_{OT} - 20}{0.8}\right) \quad (3.23)$$

Here, N, F_F , Vy *and* Iy represents the number of PV modules, fill factor, output voltage and output current of PV-module respectively. The total predictable output power (EOP) of PVGS is evaluated using (3.24) at any specific period time *t*.

$$EOP_{PV}(t) = \int_0^1 PV_{out}(s) \times f_b(s)ds \quad (3.24)$$

The hourly based mean and standard deviation of *s* is available in Table 3.1.

Table 3.1. Solar irradiance values in Tripoli [13].

Solar irradiance (kW/m^2)					
Hour	μ_s	σ_s	Hour	μ_s	σ_s
6	0.0158	0.0196	12	0.7305	0.1510
7	0.1605	0.0332	13	0.6780	0.1283
8	0.3412	0.0658	14	0.5699	0.1011
9	0.5060	0.1002	15	0.4124	0.0765
10	0.6385	0.1319	16	0.2394	0.0446
11	0.7120	0.1551	17	0.0834	0.0230

This data is adopted from Tripoli region distribution system site in the province of Tripoli, Libya [13]. The probability distribution and EOP of solar irradiance for complete 24 hours with 20 states is illustrated in Figure 3.1. Figure 3.2 represents the hourly generated output power by single PV-module.

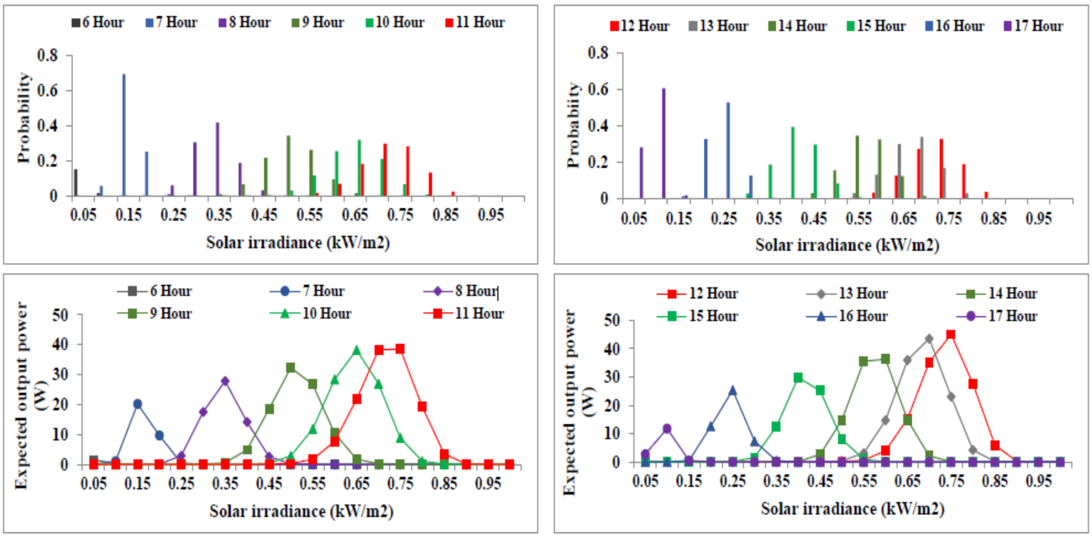

Figure 3.2. PDF values and EOP of each hour at different solar irradiance level.

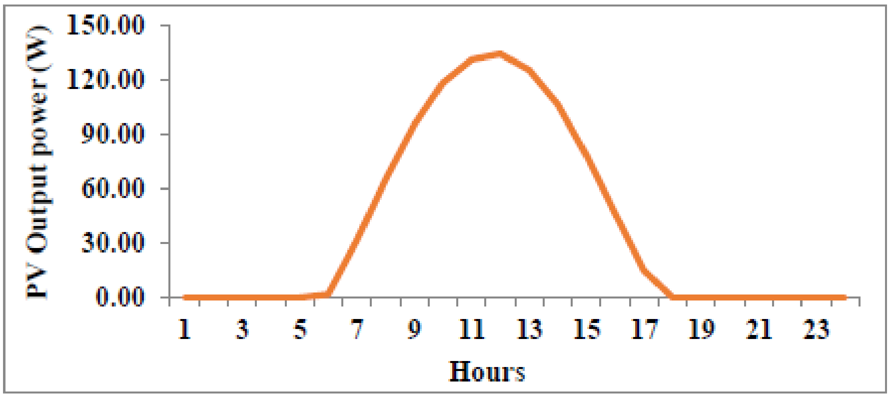

Figure 3.2. Output power of PV-module for each hour.

3.2.4. Mathematical Model of WTGS

For using of the frequency the Rayleigh probability distribution function is used [22][81]. It can be shown as equation (3.25)

$$f_w(v) = \left(\frac{2v}{c^2}\right) exp\left[-\left(\frac{v}{c}\right)^2\right] \tag{3.25}$$

Here the $f_W(v)$ is the Rayleigh PDF, c is the scale factor and v is the wind speed (see equation (3.26-3.27).

$$v_m = \int_0^{\infty} v f_w dv = \int_0^{\infty} \left(\frac{2v^2}{c^2}\right) exp\left[-\left(\frac{v}{c}\right)^2\right] dv = \frac{\sqrt{\pi}}{2} c \tag{3.26}$$

$$c \cong 1.128 v_m \tag{3.27}$$

In addition, the hourly based wind speed information has been taken from Tripoli region distribution system site in the state of Tripoli, Libya as tabulated in Table 3.2 [13].

Table 3.2. Details of wind speed [13].

Hour	$\boldsymbol{\mu_w}$	$\boldsymbol{\sigma_w}$	Hour	$\boldsymbol{\mu_w}$	$\boldsymbol{\sigma_w}$
1	9.900	0.7937	13	7.9667	0.3786
2	9.3667	0.8021	14	8.00	0.4583
3	9.1667	0.8505	15	8.00	0.500
4	9.000	0.8185	16	7.7333	0.4509
5	8.700	0.7550	17	6.9667	0.2309
6	8.600	1.0583	18	5.9667	0.3786
7	9.00	1.1533	19	4.8333	0.3215
8	9.0333	1.1504	20	4.4333	0.3215
9	9.3333	0.9504	21	4.3333	0.4163
10	9.600	1.1533	22	4.1000	0.2646
11	10.1333	1.0066	23	4.0667	0.2082
12	10.2667	0.8622	24	4.0000	0.1732

The total EOP of WTGS is evaluated using (3.29) at any specific period time t.

$$P_w(v) = \begin{cases} 0, & 0 \leq v_{aw} \leq v_{cin} \\ P_{rated} \times \frac{v_{aw}-v_{cin}}{v_{rt}-v_{cin}}, & v_{cin} \leq v_{aw} \leq v_{rt} \\ P_{rated,} & v_{rt} \leq v_{aw} \leq v_{cof} \\ 0, & v_{cof} \leq v_{aw} \end{cases} \tag{3.28}$$

$$EOP_{WT}(t) = \int_0^1 P_w(v) \times f_w(v) dv \tag{3.29}$$

The EOP of WT for different states of wind speed is determined using (3.25) -(3.29). The probability distribution and EOP of wind speed of each hour of the day with 24 states was illustrated in Figure 3.3. In addition to that, the hourly generated output power via WTGS is portrayed in Figure 3.4.

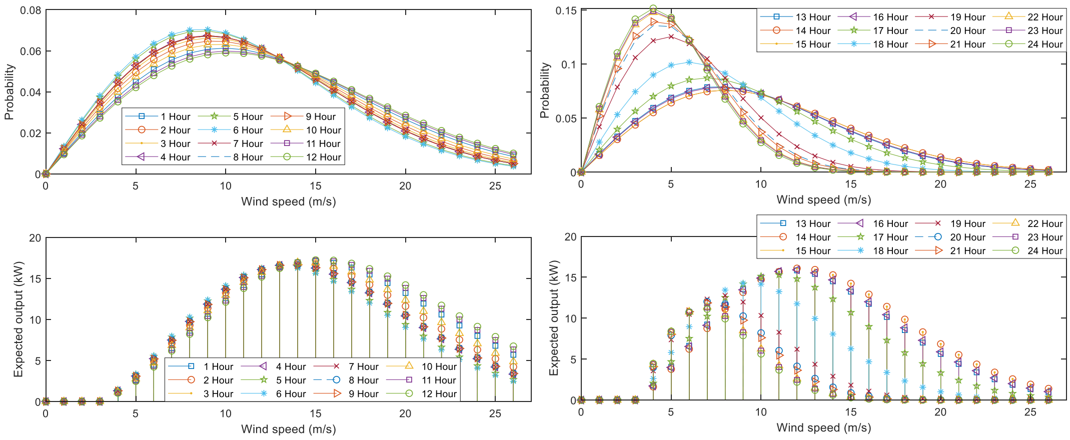

Figure 3.3. PDF values and EOP of each hour at different wind speeds**.**

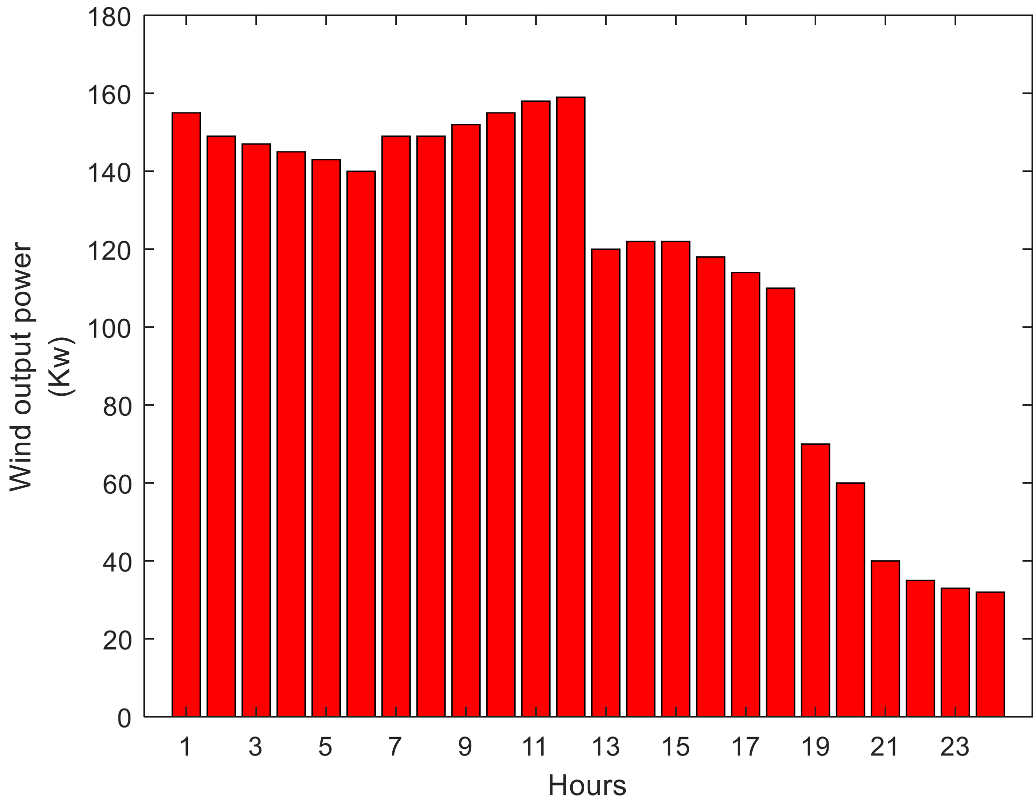

Figure 3.4. Hourly output power of WT Discharging /Charging Scheduling of EVs.

The wind turbine, PV-array and EVs technical parameter is available in table 3.3.

Table 3.3. Technical parameter for wind turbine, PV-array and EVs

Wind turbine	Cut-in speed (*vci*)		Rated speed (*vr*)		Cut-off speed (*vco*)			Capital cost (US$)	
	3 m/s		12 m/s			25 m/s	2290		
PV-array	*TA* (°C)	*NOT* (°C)	*IMPPT* (A)	*VMPPT* (V)	*ISC* (A)	*VOC* (V)	*Ki* (A/°C)	K_v (V/°C)	Capital cost (US$)
	30.76	43	7.76	28.36	8.38	36.96	0.00545	0.1278	3000
EVs	ϕmin	ϕmax	η*ch*	η*dch*	ϕ*dep*			μ_v*cap*(kWh)	
	20%	90%	85%	85%	50%		10		

In this investigation, the grid synchronized vehicles are in use as source for supplying power to grid during peak hours and during off peak hours of the grid for charging the vehicles. As per the rule of deregulated electrical energy market, the spot electrical energy cost is affirmed one day before, based on that the vehicle proprietors decide discharging and charging schedule of their vehicles to attain extreme benefit [79][80]. Hence, the discharging/charging power of grid connected vehicles for 24 hours was calculated using (3.30) and (3.31) respectively.

$$P_{dch}(t) = \mu_{vcap}[\phi_{pre} - \phi_{min}]N_{Ev(dch)}(t) \tag{3.30}$$

$$P_{ch}(t) = \mu_{vcap}[\phi_{dep} - \phi_{pre}]N_{Ev(ch)}(t) \tag{3.31}$$

Here, ϕ_{pre} & ϕ_{dep} is the current and exit state of charge. $N_{Ev(ch)}$ / $N_{Ev(dch)}$ stand for the number of EVs arriving for discharging/charging. $\boldsymbol{\mu_{vcap}}$EVs battery capacity. For extended life of EVs battery, the discharging / charging ratings should be preserved between maximum (ϕ_{max}) and minimum (ϕ_{min}) level.

$$\phi vcap_{vcap} vcap_{max_{min}} \tag{3.32}$$

3.2.5. Biomass Power Generation

Biomass is a combustible gas that is generated in natural media or in specific devices, by the biodegradation reactions of organic matter, through the action of microorganisms and other factors, in the absence of oxygen (that is, in an anaerobic environment). This gas has been called swamp gas. Biomass is obtained from organic waste, since there is a biodegradation of plant waste like that described. The processing of the biomass is shown in figure 3.5.

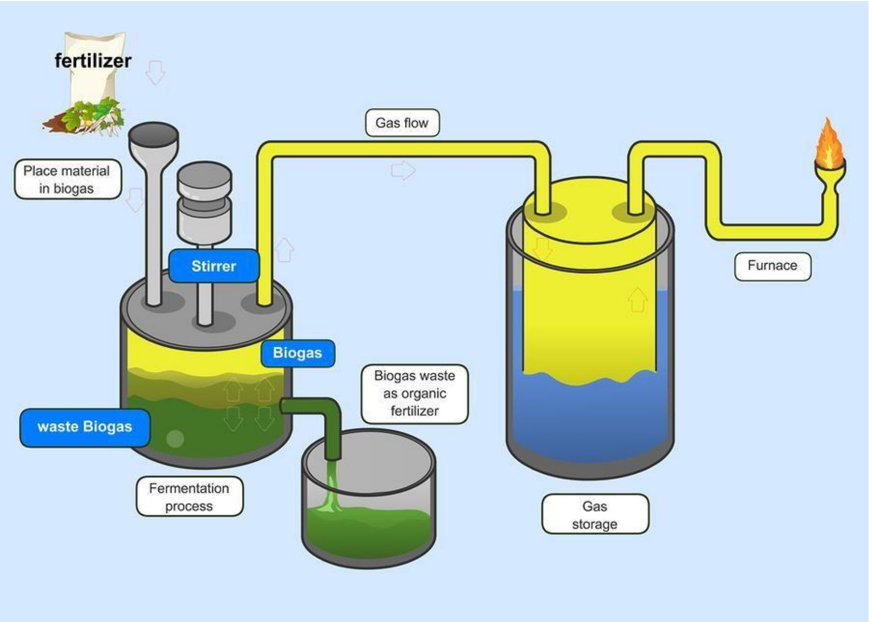

Figure 3.5. The processing of the biomass (extraction and using).

The production of biomass done by anaerobic decomposition that is a useful way of treating biodegradable waste, since it produces a valuable fuel, in addition to generating an effluent that can be applied as a soil conditioner or generic fertilizer.

The result is a mixture consisting of methane in a proportion that ranges between 50% and 70% by volume, and carbon dioxide smaller proportions of other gases such as hydrogen, nitrogen, oxygen, and hydrogen sulfide / hydrogen sulfide. Biomass has an average calorific value between 18.8 and 23.4 mega joules per cubic meter (MJ / m^3).

Biomass has an average calorific value between 18.8 and 23.4 mega joules per cubic meter (MJ / m³).

This gasoline, properly purified, can be used to supply power through turbines or gasoline generating flowers, and additionally to provide warmness in ovens, stoves, dryers, boilers, heating, or different well adapted structures.

Libya's capability of biomass is limited. Biomass power sources are small and might simplest be used on an individual stage as an energy supply. It isn't suitable to supply strength [82]. The power shortage in Libya rural areas electricity are brief, but the new rural construction is growing and growing call for power, to evaluation the resources and environment circumstance, it's far appropriate for popular the usage of biomass electricity technology generation in rural areas wherein are in animal husbandry because the financial pillar enterprise and agriculture, forestry and uncooked fabric wealthy region, thus to sell the improvement of agriculture and animal husbandry, and farmers' earning. The model is as follows formula (3.33) [83]:

$$P_{BM} = \partial_0 + \partial_1 F_1 + \partial_2 F_2 + \partial_3 F_1^2 \quad (3.33)$$

P_{BM} is the output power of biomass power generation. F_1 and F_2 are pressure and gas consumption. Their unit are kPa and NM3 / h respectively. ∂_0 is constant value. ∂_1 , ∂_2 are pressure biomass power generation and gas consumption of linear coefficient; ∂_3 is the quadratic term coefficient. For this parameter we used the data from table 3.4.

Table 3.4. Parameter that used in the biomass power generation.

Parameter	**Value**
∂_0	2338.10
∂_1	323.42
∂_2	8.46
∂_3	26.05

From equation (3.8), (3.24), (3.29) and (3.33), the total power is calculated by:

$$P_{Tot} = C_{EV}(t) + EOP_{PV} + EOP_{WT} + P_{BM} \tag{3.34}$$

After substitution (3.8), (3.24), (3.29) and (3.33) in (3.34) it can be:

$$P_{Tot} = \rho_E(t)[\eta_{dch}P_{dch}(t) - \eta_{ch}P_{ch}(t)] + \int_0^1 PV_{out}(s) \times f_b(s)ds$$
$$+ \int_0^1 P_w(v) \times f_w(v)d + \partial_0 + \partial_1 F_1 + \partial_2 F_2 + \partial_3 F \tag{3.35}$$

In this equation P_{Tot} is total power of these plants. Other items mentioned before.

3.2.6. Cost, Power Loss and Emission Optimization

An optimization method is essential to decide every judgment variable elegantly and assure all equality and inequality constraints. The use of DERs should be optimum to reduce the total expense, emissions, and power loss up to the vital value. This can only be done if the location and size of DERs are identified correctly. Therefore, multi objective crow search optimization algorithm was proposed due to its robustness and ability to search out the optimal result. In addition, the optimal locations and optimum quantity of DERs are determined under uncertain nature of load and DERs both. So, they are considered as judgment variables. Hence, it is comprehended that, this method is suitable and effective for solving this composite nonlinear multi objective problem and to achieve better outcomes [84].

3.3. REVIEW OF HONEY- BEE AND CROW SEARCH OPTIMIZATION ALGORITHM

3.3.1. Honeybee Algorithm

Bees algorithm is a search algorithm based on population and was first proposed by Karaboga [85]. During the search for food, the algorithm imitates the behavior of honey-bee swarms. In the first iteration, together with random search, the algorithm conducts a local search which can be used to simplify the problems.

The algorithm starts in the first step with (n) the scout bees being randomly positioned in the search space. Then, Finesses of scout bees visited sites are measured. In the next step, in a neighborhood search, (m) sites with the highest finesse are selected. Then The algorithm performs searches about the sites selected, assigning more bees to find the best (e) sites nearby. Choosing the best places is made directly according to their finesse. The fitness values are also used to determine the probability of picking bees. Only one bee with the highest fitness is selected for each patch in the next step to form the next population of bees. Searches of the best (e) sites in the community that represent more viable options are achieved by hiring more bees to follow them rather than the other bees. This differential recruitment, together with the scouting, is a key process of the Bees Algorithm. The remaining (m-n) bees in the population are randomly assigned around the search space in the final stage, searching for new potential solutions. Such steps are repeated until a condition of halting is fulfilled. The colony will have two sections for its new population at the end of the iteration, those which were the fittest members from a region and those which were sent out randomly [85].

3.3.2. Crow Search Algorithm

Askarzadeh has been developed Crow Search Algorithm (CSA) [86], which simulates the behavior of crow to search food and share the knowledge of food to neighbor crow. It is most intelligent animal in the world [86]. Thus, their behaviors offer attractive heuristics. Crow search algorithm is stimulated via the robbery activities to facilitate crows reveal; such activities are categorized as follows: memory behavior of the crow to hide expedient food, crow can communicate with other crow to follow to robbery the food [87]. The crow can move randomly to mislead the opponent to protect the food from others.

From the mathematical calculation analysis, in the CSA the group $C^K(\{C_1^K, \quad C_2^K, \quad \cdots, \quad C_N^K\})$ of N folks (crows) is developed from preliminary point (K=0) to a maximum value of generations (K= total no iteration). Every crow $C_i^K(i\epsilon[1,\cdots,N])$ characterizes a d-dimensional vector $\left\{C_{i,1}^K \quad C_{i,2}^K \quad \cdots \quad C_{i,N}^K\right\}$ where every measurement matches to an assessment parameter of the problem of the controller to be resolved. In Crow search algorithm, a new group C^{K+1} is created in view of two states: the first is while the crow is conscious that is start follow and the next is while the crow is not conscious. A consciousness possibility factor AP_i^K decides which condition is chosen. Every original constituent can be computed as follows:

$$C_i^{K+1} = \begin{cases} C_i^K + r_i \times fl \times \left(m_j^K - C_i^K\right) & r_j \geq AP_i^K \\ random\, position & otherwise \end{cases} \tag{3.36}$$

Where, r_i and r_j are homogeneously distributed arbitrary number between 0 and 1, limit of control the flight length is denoted by fl. The remembrance of the crow j at iteration K is denoted by m_j^K; it supplies the paramount position created so distant by the crow j. CSA only need the pattern of two limits, AP_i^K and fl as well, the updating equation is relatively easy, providing an easy to use yet powerful realization.

The necessary ladders of CSA are shown in the flowchart of figure 3.5. The first step is the defining of the objective (size and constrain) and the factors of the CSA (fl AP, stop criteria). The subsequently step consists in arbitrarily initialize the crow locations and calculated them using the fitness function. The location is uniformly spread in the explore space. After that, the new locations are generated according to equation (3.31a) and their possibility is confirmed. All the new locations are calculated in the fitness function, and the memory is updated. Lastly, the stop condition is verified to end or continue with the iterative procedure. The stop condition depends on the execution of the CSA, but two universal rules are used: 1) the use of a predefined number of iterations and 2) when the fitness function value of the most excellent crow converges and does not change along the iterations.

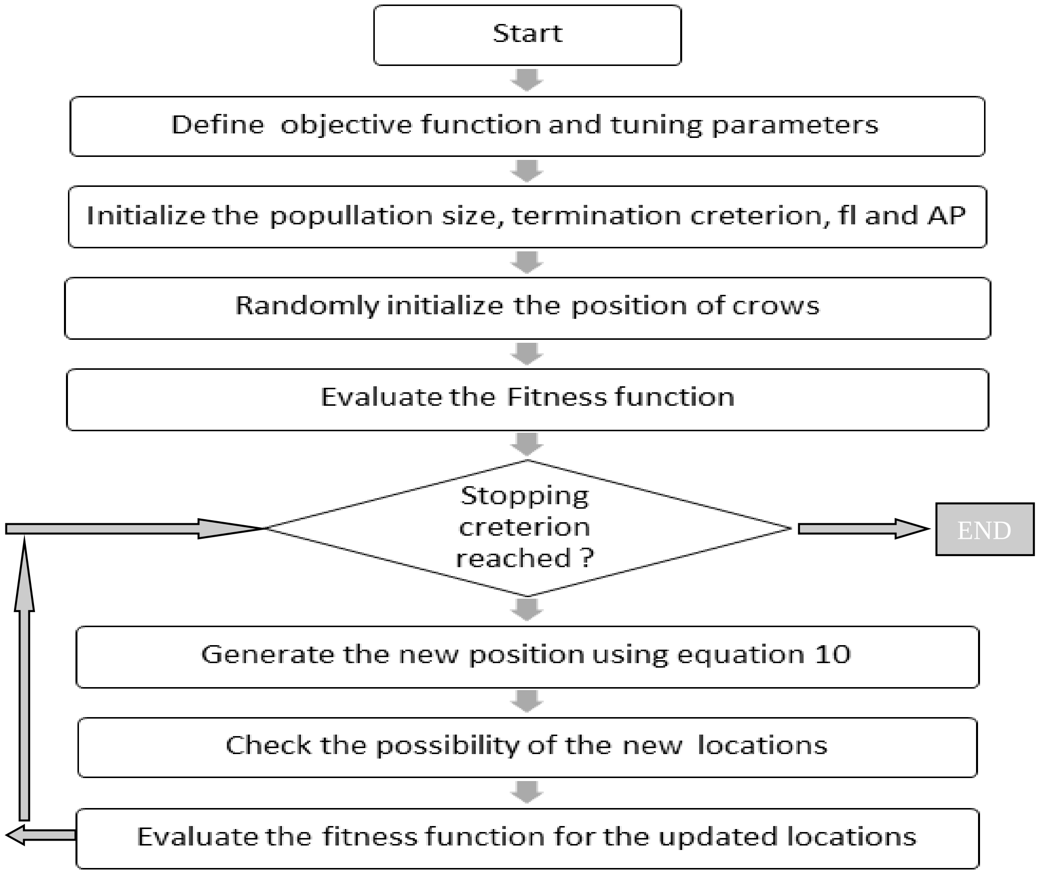

Figure 3.6. Flowchart for the crow search algorithm.

CSA reach global minimum point quickly than another optimization algorithm. This algorithm not trap in the local minimum point. This algorithm provides accurate results than another optimization algorithm.

By simulating the intelligent behavior of crows, CSA tries to find optimal solutions to various optimization problems. It has gained a considerable interest worldwide since its advantages like simple implementation, a few numbers of parameters, flexibility, etc.

- Simplicity, flexibility, robustness, scalability, and self-organization.
- Few control parameters as compared to Evolutionary Algorithm (EA).
- Execution of various tasks by individuals simultaneously.
- Memory space is less utilized by swarm intelligence (SI) compared to EA.

3.4. IMPLEMENTATION OF CSA ALGORITHM FOR SOLVING OPTIMAL DERS INTEGRATION PROBLEM

In this work, the CSA optimization technique is utilized for solving optimal DERs installation task to reduce the power loss, total expense i.e., cost of purchase active power, WTGS installation, WTGS O&M, PVGS installation, PVGS O&M, EVs charging/discharging along with emissions produced through power plants. The optimal strategy that has been used here for finding out the better solution may be represented as

$$K^1 = [WT^1 \quad PV^1 \quad EV^1] \tag{3.37}$$

Here, K^1 is a vector. WT^1, PV^1 and EV^1 are the thirty-one-column matrix may be expressed as

$$K^1 = \left[\underbrace{WT_{loc1}^1 \quad PV_{loc1}^1 \quad PV_{loc2}^1 \quad EV_{loc1}^1}_{Location\ of\ WT,\ PV\ \&\ EVs} \quad \underbrace{WT_{No.1}^1 \quad PV_{No.1}^1 \quad PV_{No.2}^1 \quad EV_{No.1}^1 \ldots\ldots EV_{No.24}^1}_{Number\ of\ WT,\ PV\ \&\ EVs} \right] \tag{3.38}$$

Where WT^1_{loc1}, PV^1_{loc1}, PV_{1loc2}, EV^1_{loc1} are the initial locations of WTGS, PVGS and EVs respectively, $WT^1_{No.1}$, $PV^1_{No.1}$ $PV^2_{No.2}$ represents the number of WTGS units and PV modules, $EV^1_{No.1}$ .... $EV^1_{No.24}$ indicates the number of grids connected vehicles arriving for charging/discharging purpose along 24 hours. These variables are considered as decision variables during optimization process. By upgrading the solution search equations of CSA technique, the q^{th} solution set is generated through the new decision variable i.e., locations and number of WTs, PVs and EVs as follows.

$$K^q = [WT^q \quad PV^q \quad EV^q] \tag{3.39}$$

For each q^{th} solution, B/F load flow program is executed and compute fitness function value. The obtained function value was compared with the previous solution values, healthier outcome is chosen and discards worst.

In this thesis, for Photovoltaic Generation System (PVGS), Wind Turbine Generation System (WTGS), and Electric Vehicles (EVs) in supply network simultaneously an optimal integration of (DER) designed and implemented for motive of abatement of overall power loss, overall cost and emanations dispatched through the thermal generators. To accomplish these planned purposes and profits, we designed a multi-objective function. PVGS and WTGS numerical model actualize for registering the likelihood of wind speed and sun-based irradiance. So that, the normal yield force can be assess. In addition, the charging/discharging concepts of EVs also consider in this work.

Dervis Karaboga [88] suggested that meta-heuristic optimization bee colony optimization (BCO) being able to solve certain problems, combinatorics, and also issues is characterized by a combination of uncertainty. A bee colony can be spread over long distances as well as in different directions to take advantage of food sources. Flowering parts with large amounts of nectar and pollen, which can be collected with little effort, are visited by many bees; So that the parts of the earth that have less pollen or nectar attract less bees. The process of searching for food in a colony is initiated by watch bees, which are sent in search of promising flowers. Watch bees move from one flowerbed to another. During the harvest season (flowering), the colony continues to search for several colony populations as watch bees. When the search for all the flowers is over, each watch bee performs a special dance on top of the flower, which has a reliable supply of nectar and pollen. This dance, known as the spin dance, transmits information about the direction of the flower bed (relative to the hive), the distance to the flower garden, and the quality of the flower garden to other bees. Most follower bees go to flowerbeds where there is more hope and there is more hope of finding nectar and pollen. When all the bees have moved to the same area, they are again randomly scattered around the flowerbed due to the extent of their dance, so that eventually not one flowerbed, but the best flowers in it are positioned [88][89][90][91]. The equation for this aim can be represented as following equations.

$$Z_{i,j} = y_{i,j} + \sigma_{i,j} \cdot \left(y_{i,j} - y_{k,j}\right) \tag{3.40}$$

$$P_i = \frac{F_i}{\sum_{j=1}^{SR} F_j} \tag{3.41}$$

$$y_{i,j} = LB_{i,j} + rand(0,1) \cdot \left(UB_{i,j} - LB_{i,j}\right) \tag{3.42}$$

The creation power age by means of PV module mainly relies on the convergence of sun-oriented irradiance. The hourly irradiance episode at a fixed spot for the most part they expect a binomial allotment, it is a variety of two straight unit-modular circulation capacities [19][20]. A beta Probability Density Function (PDF) is created to both unit-modals, as set out in the accompanying:

$$f_b(s) = \begin{cases} \frac{\Gamma(\alpha+\beta)}{\Gamma(\alpha)+\Gamma(\beta)} \times s^{(\alpha-1)}(1-s)^{(\beta-1)} & for\ 0 \le s \le 1,\ \alpha \ge 0,\ \beta \ge 0 \\ 0 & otherwise \end{cases} \tag{3.43}$$

Here, s represents the sun powered irradiance (kW/m2). α and β are the beta conveyance work fb(s) boundaries, these can be determined utilizing (3.44) and (3.45).

$$\beta = (1-\mu_s) \times \left(\frac{\mu_s \times (1+\mu_s)}{\sigma_s^2} - 1\right) \tag{3.44}$$

$$\alpha = \frac{\mu_s \times \beta}{1-\mu_s} \tag{3.45}$$

For producing the PDF, the entire day is part into 24-hour timeframe. Consistently having own PDF as per the sun powered irradiance. According to the recorded information, the hour savvy μ_s and σs of the day are assessed. It is viewed as that consistently having 20 conditions of s with a stage of 0.05 kW/m2. From μ_s and σ_s values, the PDF of every hour of the day with 20 states is resolved utilizing. As per that, the yield force of PVGS (PV_{out}) is resolved for that specific hour utilizing (3.46) [20].

$$PV_{out}(s) = N \times F_F \times V_y \times I_y \quad (3.46)$$

$$V_y = V_{oc} - V_k \times T_{cy} \quad (3.47)$$

$$I_y = s[I_{sc} + I_k(T_{cy} - 25)] \quad (3.48)$$

$$F_F = \frac{V_{MPT} \times I_{MPT}}{V_{oc} \times I_{sc}} \quad (3.49)$$

$$T_{cy} = T_A + s\left(\frac{N_{OT} - 20}{0.8}\right) \quad (3.50)$$

The parameter that used in crow search algorithm is shown in table 3.5.

Table 3.5. the parameter that used in crow search algorithm.

No.	**Parameter**	**Description**	**Value**
1	nVar	Number of Decision Variables	8
2	nPop	Population Size	100
3	LB	Lower Bound of Variables	[50 1 0 0.5 0.5 0.5 0.5 0.5]
4	UB	Upper Bound of Variables	[300 15 10 0.9 0.9 0.9 0.9 0.9]
5	MaxIter	Number of Iteration	1000
6	fl	Flight length	20
7	AP	Awareness probability	0.00001

The parameter that used in Honeybee algorithm is shown in table 3.6.

Table 3.6. the parameter that used in Honey Bee algorithm.

No.	**Parameter**	**Description**	**Value**
1	nScoutBee	Number of Scout Bees	30
2	nSelectedSite	Number of Selected Sites	15
3	VarMin	Lower Bound of Variables	[50 1 0 0.5 0.5 0.5 0.5 0.5]
4	VarMax	Upper Bound of Variables	[300 15 10 0.9 0.9 0.9 0.9 0.9]
5	MaxIter	Number of Iteration	40
6	nEliteSite	Number of Selected Elite Sites	6
7	nSelectedSiteBee	Number of Recruited Bees for Selected Sites	15
8	nEliteSiteBee	Number of Recruited Bees for Elite Sites	30
9	r	Neighborhood Radius	[25 1.4 1 0.04 0.04 0.04 0.04 0.04]
10	rdamp	Neighborhood Radius Damp Rate	0.95

CHAPTER 4

EXPERIMENTAL RESULT

4.1. RADIAL DISTRIBUTION FEEDER

The proposed integrated approach was simulated on 11 kV, 28-bus practical rural ring distribution feeder for abatement of total cost, total power loss and emissions. This test system consists of 28-buses, 27-branches, one main distribution segment connected with five laterals. Base MVA of this system is 100 and operated at 11 kV [82]. The single line representation of this test feeder is displayed in Figure 4.1. This test system is located at zone (32°54'N and 13°11'E) in the province of Tripoli, Libya. It is associated with the three different genre of customers i.e. commercial residential and industrial at different load buses [83][92]. This uncertain load demand of each bus for 24 hours is displayed in Figure 4.1. Moreover, the spot electricity market price for each hour which is taken from Libyan Energy Exchange [93].

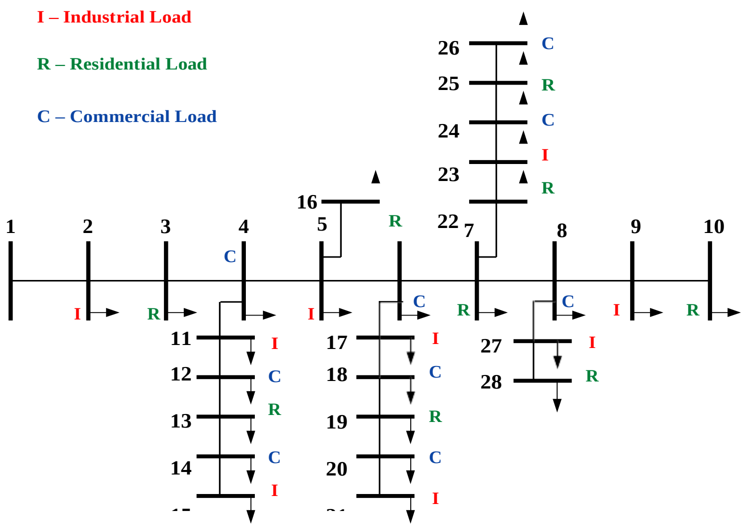

Figure 4.1. Bus practical radial distribution feeder.

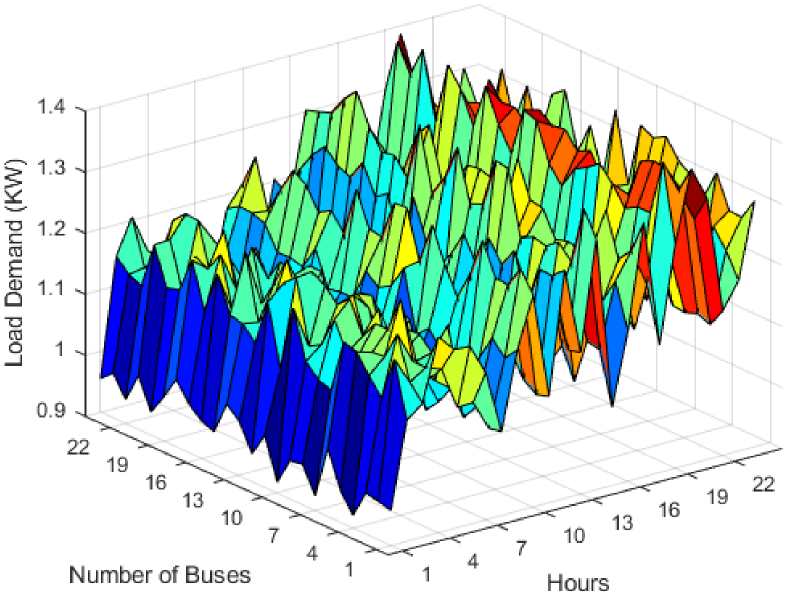

Figure 4.2. Uncertain load demand of each bus of the distribution network for 24 hours.

As per IEEE 1547 standard, the renewable energy sources should operate at fixed power factor which is closer to the unity with respect to the electrical power network. Many electrical power utilities and independent power producers have decided that renewable power source can operate at maximum 0.95 operation mode. Furthermore, analyze the impact of renewable power sources by varying the power factor therefore, various cases have been considered, as indicated in Table 4.1. Furthermore, the cost specifications of WTGS and PVGS were calculated [78]. The technical specification of WTGS, PVGS and EVs are designed [94] The simulation was completed on MATLAB/Simulink platform (R2019) In addition, the case wise exhaustive discussions on simulation results are discussed as follows:

Table 4.1. Various cases for simulation analysis.

Cases	Explanation
1	Without any DERs integration (base case)
2	Optimal integration of WTGS, PVGS and EVs in distribution system. WTGS and PVGS operating at 0.95 leading power factor
3	Optimal integration of WTGS, PVGS and EVs in distribution system. WTGS and PVGS operating at unity power factor
4	Optimal integration of WTGS, PVGS, EVs, and Biomass in distribution system. WTGS and PVGS operating at 0.95 lagging power factor

4.2. CASE 1

This is the base case of the considered test scheme without DERs integration. The basic B/F load flow has been executed to evaluate the active as well as reactive power loss, bus voltage and line current value of the feeder. The reactive and active power loss of this test feeder is 371.87 "kVAr" and 554.55 kW respectively. In addition, the cost of active power purchase from grid is 370625073.00 US$ correspond to emission dispatched through power plant is 20952.00 "lb/kWh".

4.3. CASE 2

In this case, both renewable power sources i.e., PVGS and WTGS insert active power and absorb reactive power to/from the network. These DERs are established at the same time in distribution system at best allocations. The optimal location and rating of WTGS is bus number 4 and 1 unit of 250 kW correspondingly. In the same way, the best location and rating of PVGS is bus number 5 and 62.92 kW correspondingly. Bus number 6 is the optimal bus to charge/discharge EVs battery. Hour wise generated output power by PVGS is indicated in Figure 4.3(a). The number of vehicles arriving for charging/discharging is shown in Figure 4.3(b). The obtained simulation results after DERs integration are indicated in Table 4.2 and Table 4.3. The reactive and active power loss becomes 279.45 kVAr and 419.70 kW respectively and total power loss reduction is 24.32 %. Moreover, the purchased real power cost from grid becomes 177206488.21 US$. The expenditure of installation of WTGS and its O&M is 29310937.50 US$ and 41528029.36 US$ correspondingly. In the same way, the expenses related to installation of PVGS, and its O&M is 7361640.00 US$ and 4172018.07 US$ correspondingly. The level of emission generation is reduced notably, and it becomes 10786.20 lb/kWh. Furthermore, for solving this problem CPU takes around 5359.23 seconds to search out the fitness value including load flow program.

4.4. CASE 3

In this case, both renewable power sources i.e., PVGS and WTGS inject active power into network. Moreover, grid connected vehicles are also incorporated for charging and discharging purpose. During charging mode these vehicles behaves as a load while in discharging mode, they supply power to the system and treated as a DG. These DERs have been located optimally in distribution system via CSA technique for the intension of deduction of total cost, power loss and emission generation level simultaneously. The optimal bus and rating of WTGS is 21 and 2 units of 250 kW. Similarly, an optimal location of PVGS is bus number 9 and 11 and respective rating is 61.16 kW and 148.72 kW respectively. Hour wise generated output power by PVGS-1 and PVGS-2 are indicated in Figure 4.3(c) and the number of gradable vehicles incoming for discharging/charging is illustrated in Figure 4.3(d). Bus number 16 is the best bus for charging/discharging of vehicles battery. At any time, these grids connected can either be discharge or charge but not both done at the same time. The idea of vehicle power generation at each hour is generated arbitrarily and the boundary of these in between 1 to 100. In this context, Table 4.2 represents the simulation outcomes after integration of DERs. Both real and reactive power loss reduced appreciably, and they become 348.57 kW and 228.85 "kVAr" respectively. The total power loss reduction is 37.14 %. In addition, the voltage level of each bus is improved notably as compared to case 1. The optimal location and size of these DERs are furnished in Table 4.3.

In cost analysis portion, the cost of purchase active power through grid gets reduced significantly by incorporating DERs and it becomes 119623672.45 US$. The cost of WTGS installation and its O&M is 58621875 US$ and 83056058.72 US$ respectively. Similarly, the cost of PVGS installation and its O&M are 24555960.00 US$ and 13916451.87 US$ respectively. The computational time of CPU is around 4379.50 seconds to seek out the solution value including load flow program.

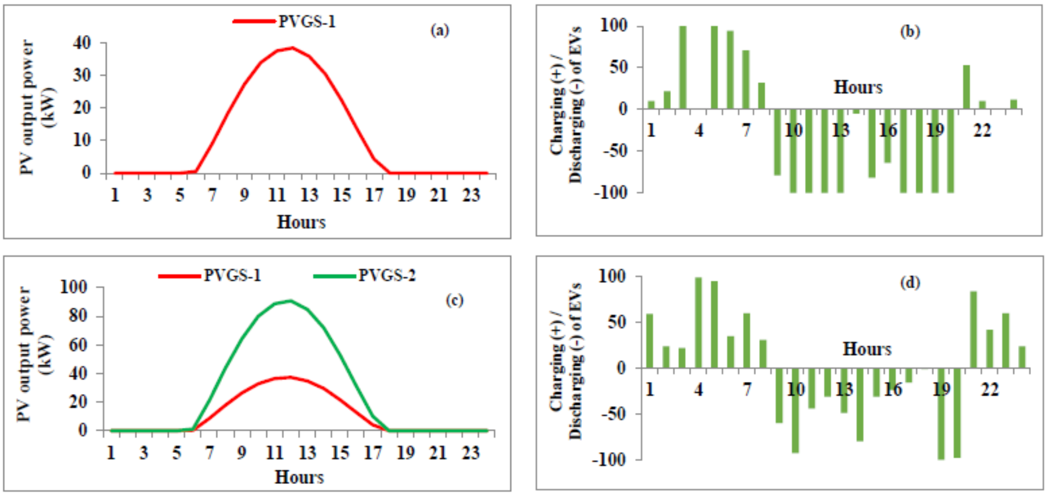

Figure 4.3. (a) Hour wise generated output power by PVGS-1 for case 2, (b) Vehicles arriving for charging/discharging at each hour for case 2, (c) Hour wise generated output power by PVGS-1 and PVGS-2 for case 3, (d) Vehicles arriving for charging/discharging at each hour for case 3.

4.5. CASE 4

In this case, both PVGS and WTGS inject active as well as reactive power to the distribution feeder. The optimal location and rating of WTGS is bus number 6 with 2 units of 250 kW. Similarly, the optimal locations of PVGS are 11 and 22 and respective ratings on these buses are 340.12 kW and 309.98 kW respectively. Bus number 2 is the optimal bus to charge/discharge EVs battery. Hour wise generated output power by PVGS and the number of vehicles arriving for charging/discharging purpose for each hour is portrayed in Figure 4.4(a) and Figure 4.4(b) respectively. The detailed numerical outcomes are seen in Table 4.2. After DERs integration, the real and reactive power loss becomes 225.81 kW and 148.90 "kVAr" respectively. The total power loss reduction is 59.28 %. Moreover, the voltage level of each bus is improved significantly to a great extent as compared to other cases. In addition, hourly based voltage profile comparison of each bus is portrayed in Figure 4.5 for case 4. The optimal locations and sizes of DERs for this case are indicated in Table 4.3. In cost analysis portion, the cost of purchase active power from grid is reduced appreciably and it becomes 77278850.15 US$. The cost of WTGS installation and its O&M is 57720000.00 US$ and 81778273.20 US$ respectively. Similarly, the cost of PVGS installation and its O&M is 74891520.00 US$ and 42442821.78 US$

respectively. Furthermore, the evaluation time of CPU to find optimal fitness function value is around 4449.13 seconds for 100 cycles including load flow program.

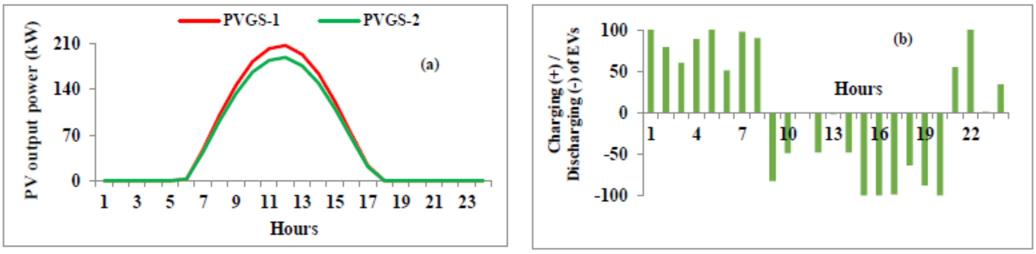

Figure 4.4. (a) Hour wise generated output power by PVGS-1 and PVGS-2 for case 4, (b) Vehicles arriving for charging/discharging at each hour for case 4.

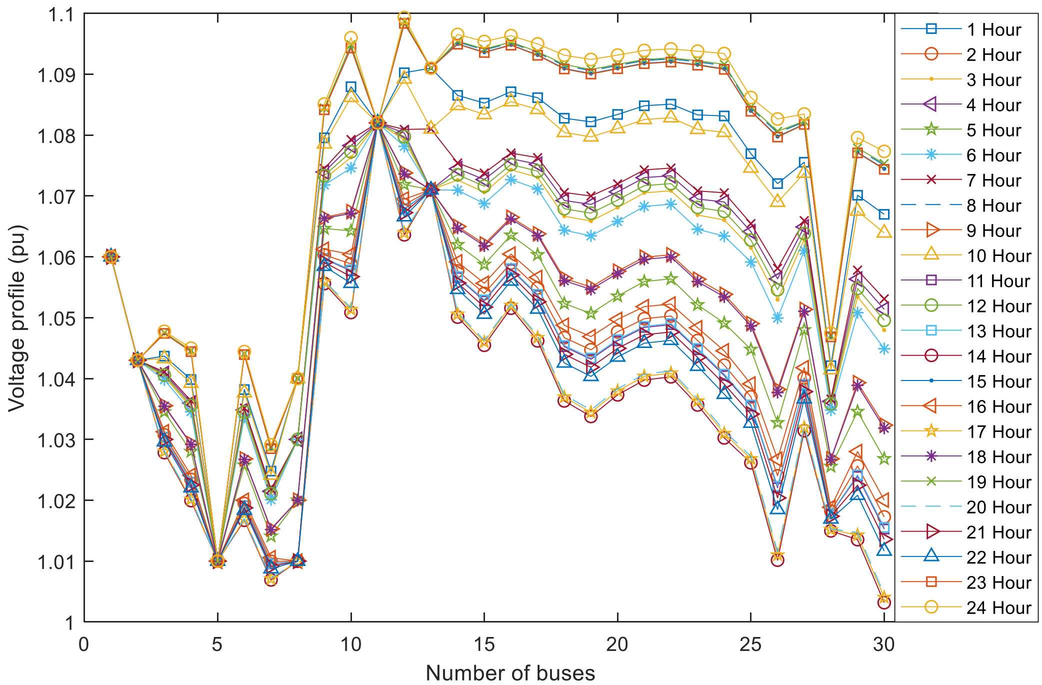

Figure 4.5. Voltage profile of case 4 during 24-hours.

Table 4.2. Simulation results of all cases before and after DERs integration.

Cases	Cases 1		Cases 2		Cases 3		Cases 4	
	CSA	HBA	CSA	HBA	CSA	HBA	CSA	HBA
∑Ploss (kW)	554.55	575.21	419.70	554.30	348.57	395.49	225.81	251.94
% Ploss Reduction	-	-	24.32	32.12	37.14	42.14	59.28	66.14
∑Qloss (kVAr)	371.87	379.15	279.45	290.14	228.85	278.85	148.90	161.27
∑ Purchased real Power cost ($) $x10^5$	3706.25	3766.58	1772.06	1814.14	1196.23	1215.54	772.78	812.36
WT installation cost ($) $x10^5$	-	-	293.10	310.14	586.21	598.37	577.20	599.12
WTO & M cost ($) $x10^5$	-	-	415.28	435.54	830.56	843.94	817.78	895.55
PV installation cost ($) $x10^5$	-	-	73.61	75.25	245.55	256.32	748.91	797.48
PV O&M cost ($) $x10^5$	-	-	41.72	43.21	139.16	143.58	424.42	447.25
Biomass installation cost ($) $x10^5$	-	-	164.23	173.13	1252.54	1232.12	1724.21	1734.41
Biomass O&M cost ($) $x10^5$	-	-	145.32	143.45	1159.24	1144.28	1422.47	1423.21
∑Emission (lb/kWh)	20952.00	21672.00	10786.20	11482.20	7030.67	7274.75	4884.50	4976.45

Table 4.3. Optimal location and size of various DERs for different cases.

Cases	Bus Number	Type of DER	Number of PV modules / WT units/EV/Biomass	Total size (kW)
Case 2	Bus-4	WTGS	1	1 x 250 =250 kW
	Bus-5	PVGS-1	286	62.92 kW
	Bus-7	EVGS	Hourly change	30 kW
	Bus-10	BioGS	1	1 x 200 =200 kW
Case 3	Bus-9	PVGS-1	278	61.16 kW
	Bus-11	PVGS-2	676	148.72 kW
	Bus-21	WTGS	2	2 x 250 =500 kW
	Bus-7	EVGS	Hourly change	30 kW
	Bus-10	BioGS	2	2 x 200 =400 kW
Case 4	Bus-6	WTGS	2	2 x 250 =500 kW
	Bus-11	PVGS-1	1546	340.12 kW
	Bus-22	PVGS-2	1409	309.98 kW
	Bus-7	EVGS	Hourly change	30 kW
	Bus-10	BioGS	3	3 x 200 =600 kW

From the achieved numerical outcomes, it is noted that case 4 gives the preferable outcomes in comparison with the other considered test cases. And, for all cases, crow search algorithm has better performance parameter such as less emission cost, less installation cost for PV and wind, less operation and maintenance cost, and less purchase real power cost when compared to honey-bee algorithm.

Hourly based impact on distribution network also has been analyzed for each case after DERs integration.

The results that obtain from the HBA is shown in following figures. The real and reactive power loss comparison between all cases is illustrated in Figure 4.6(a) and Figure 4.6(b) respectively. Similarly, the active power purchase cost and voltage deviation for each case along 24 hours are depicted in Figure 4.6 (c) and Figure 4.6 (d) respectively.

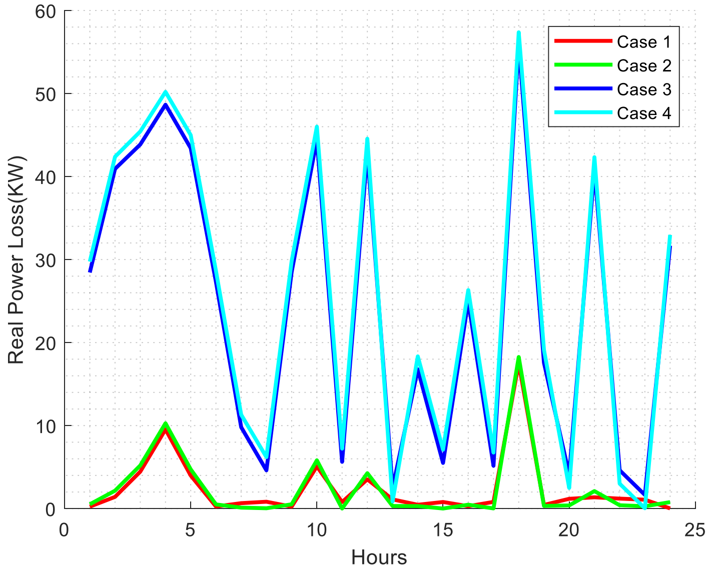

(a)

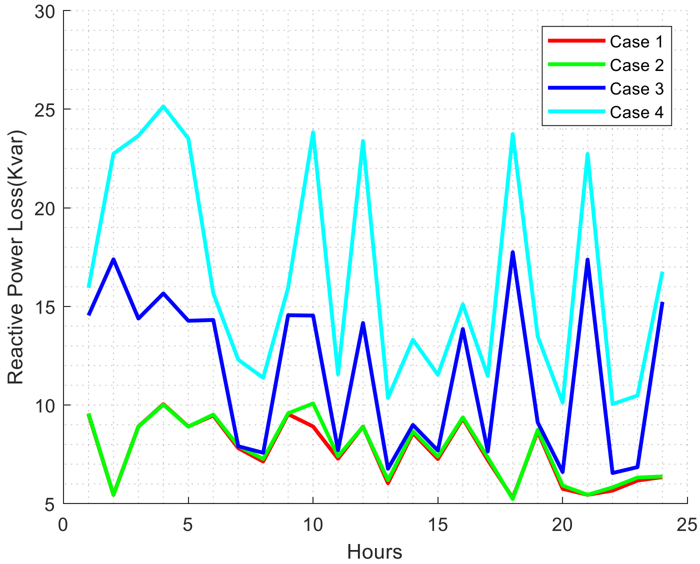

(b)

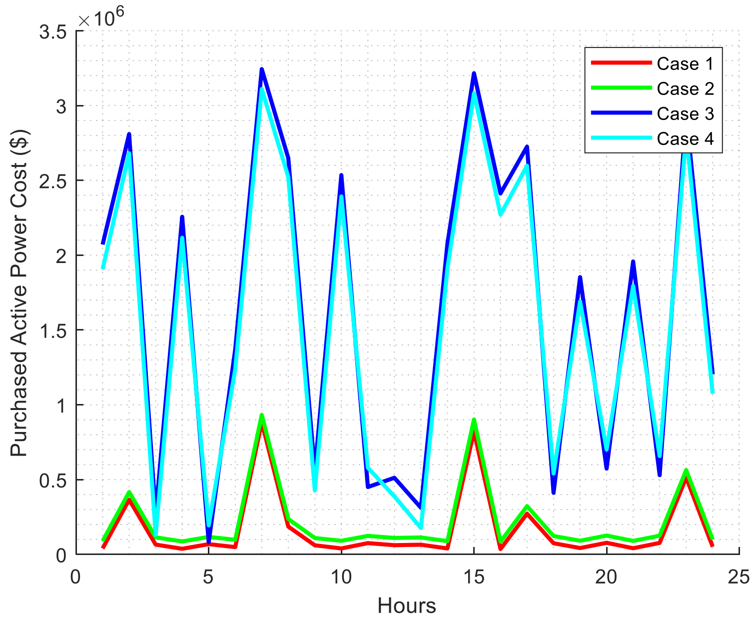

(c)

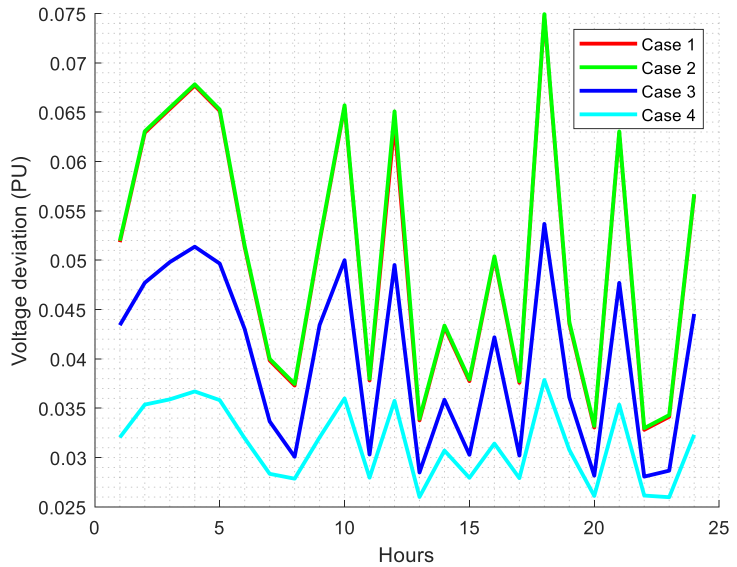

(d)

Figure 4.6. (a) Real power loss during 24 hours after DERs integration, (b) Reactive power loss during 24 hours after DERs integration, (c) Purchase active power cost from grid during 24 hours after DERs integration, (d) Voltage deviation during 24 hours after DERs integration.

In this part, the impact of PVGS, WTGS and EVs on 28-transport for dispersion framework have been researched. Accordingly, the proposed joined technique has been exhibited on 11 kV, 28-transport pragmatic country ring appropriation feeder for decrease of all out cost, all out power misfortune and emanations. This test framework comprises of 28-transports, and furthermore 27-branches, one principal appropriation fragment associated with five laterals. Base MVA of this system is 100 and operated at 11 kV [82].

Moreover, the spot electricity market price for each hour which is taken from Energy Exchange [93]. The 28- bus practical radial distribution feeder is shown in figure 4.7.

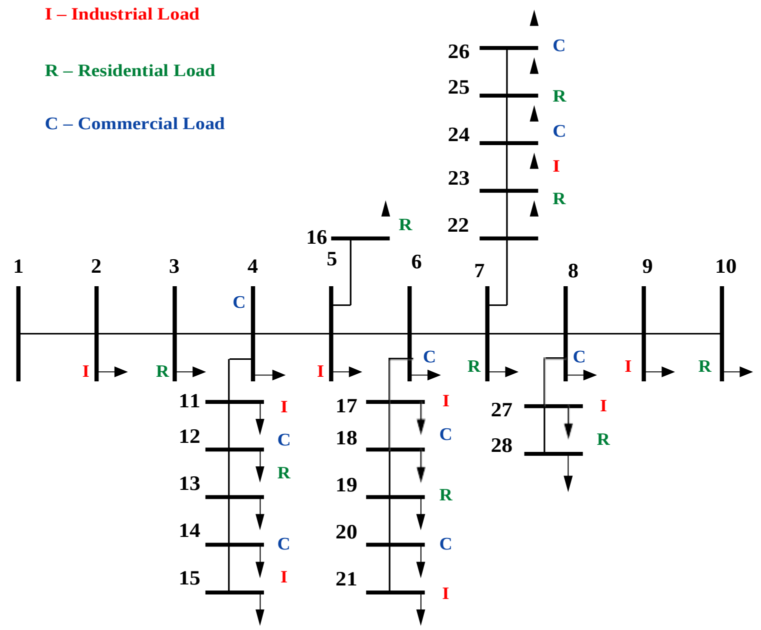

Figure 4.7. 28- bus practical radial distribution feeder.

This relationship is related to three different types of customers: commercial, residential and industrial [83] [92] in different freight buses. This uncertain 24-hour load demand for each bus is shown in Figure 4.8.

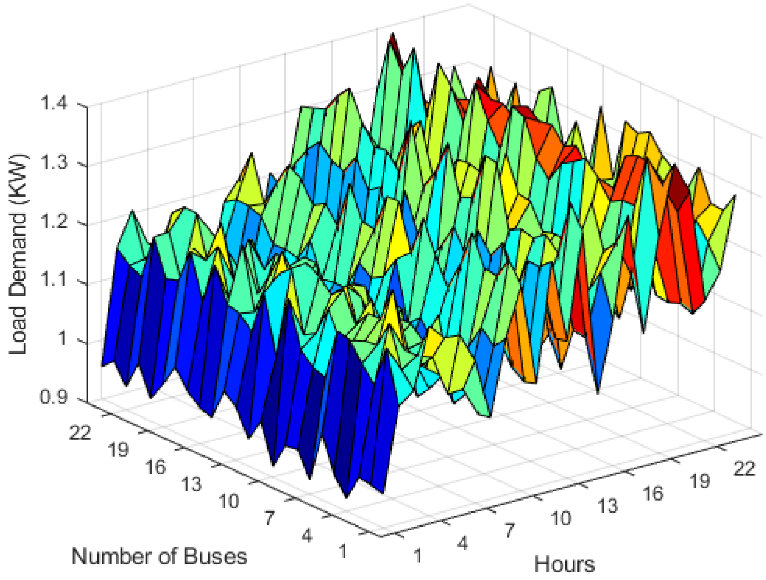

Figure 4.8. Uncertain load demand of each bus of the distribution network during 24. Hoursz.

The best cost against of the iteration number is shown in Figure 4.9.

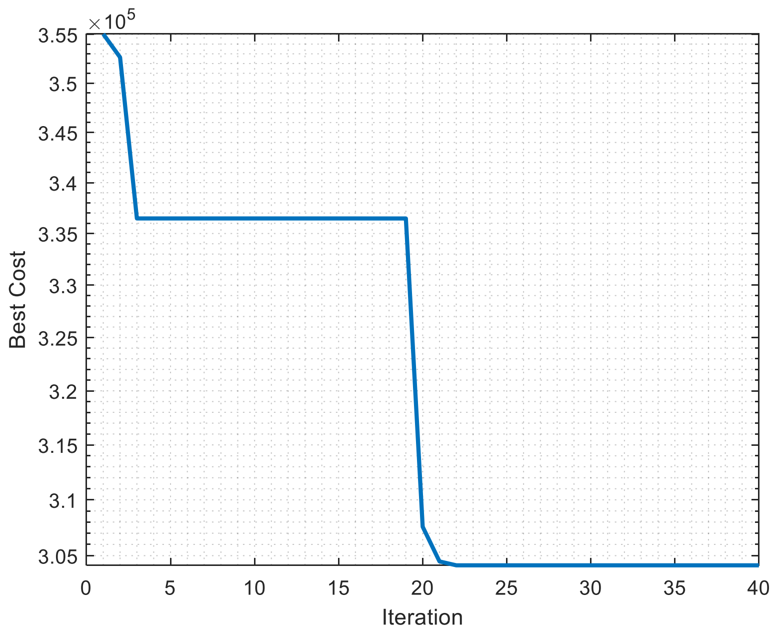

Figure 4.9. Best cost vs iteration.

The voltage profile against of the number of buses during 24-hours is shown in figure 4.10.

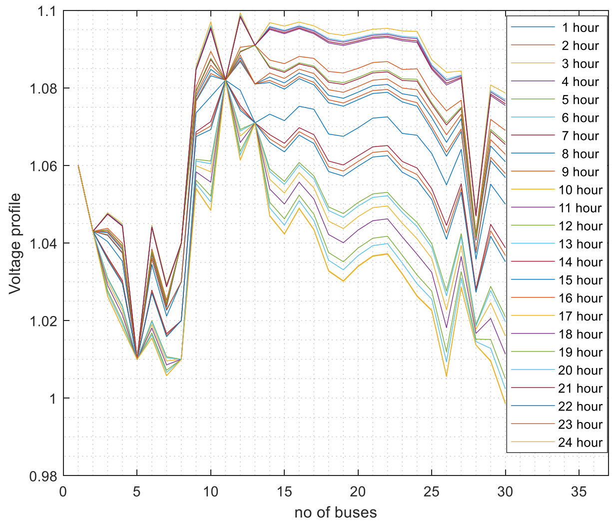

Figure 4.10. Voltage profile vs. number of buses during 24-hours.

Results taken from the CSA are presented below.

The real power loss (kW) against of the hours is shown in figure 4.11.

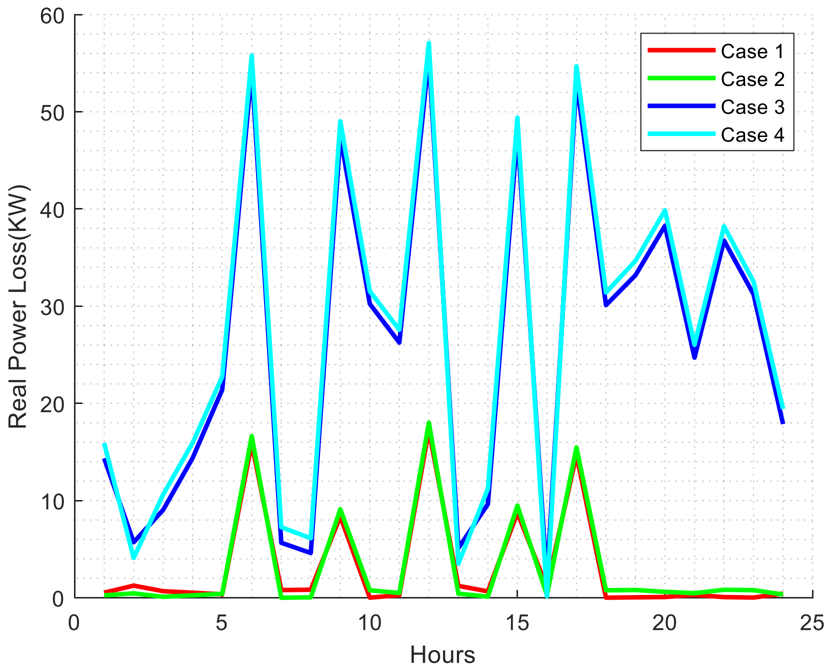

Figure 4.11. Real power loss (kW)over time plot.

Figure 4.12 shows reactive power loss (kVAR) over time.

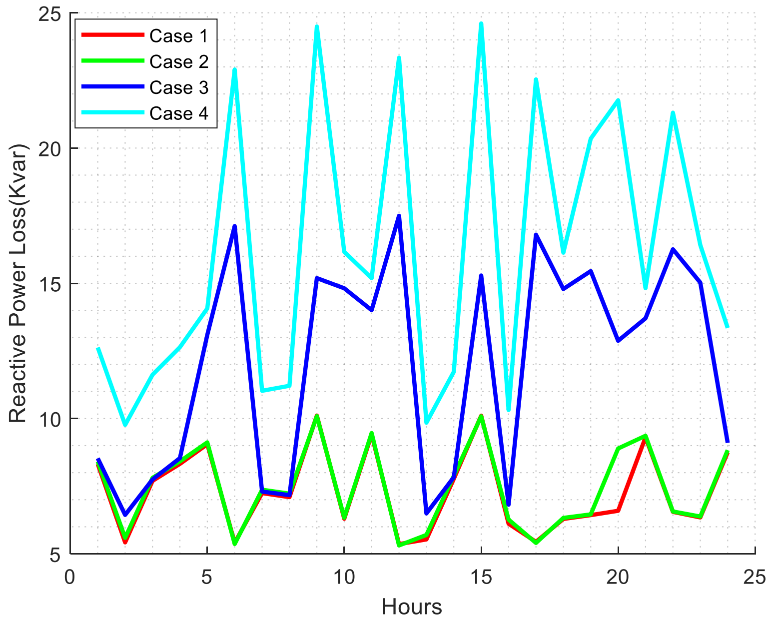

Figure 4.12. Reactive power loss (kVAR)-time plot.

Figure 4.13 shows the purchased active power cost loss ($) - time.

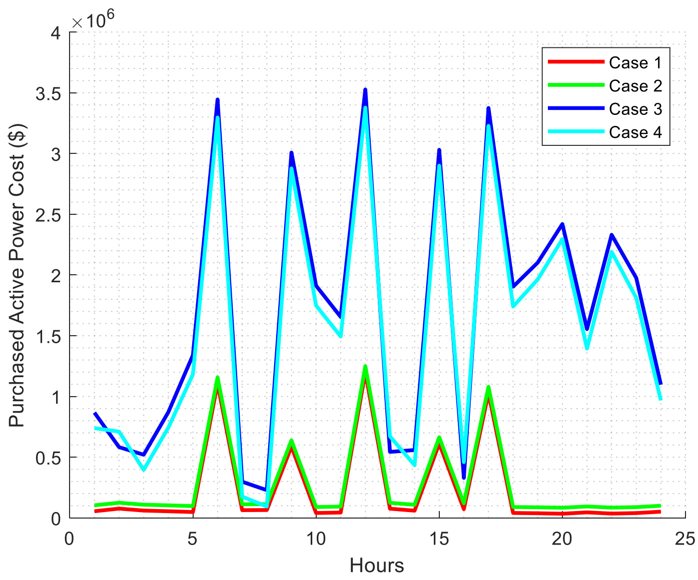

Figure 4.13. Purchased Active Power Cost loss ($) - time plot.

Figure 4.14 Voltage deviation (PU)-time plot.

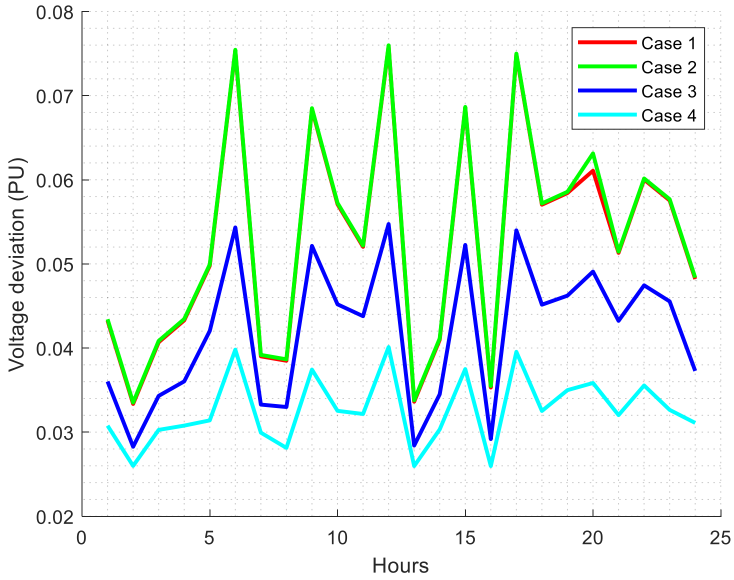

Figure 4.14. Voltage deviation (PU) vs. Hours.

The simulation results for all cases before and after DER implementation shown in figure 4.15.

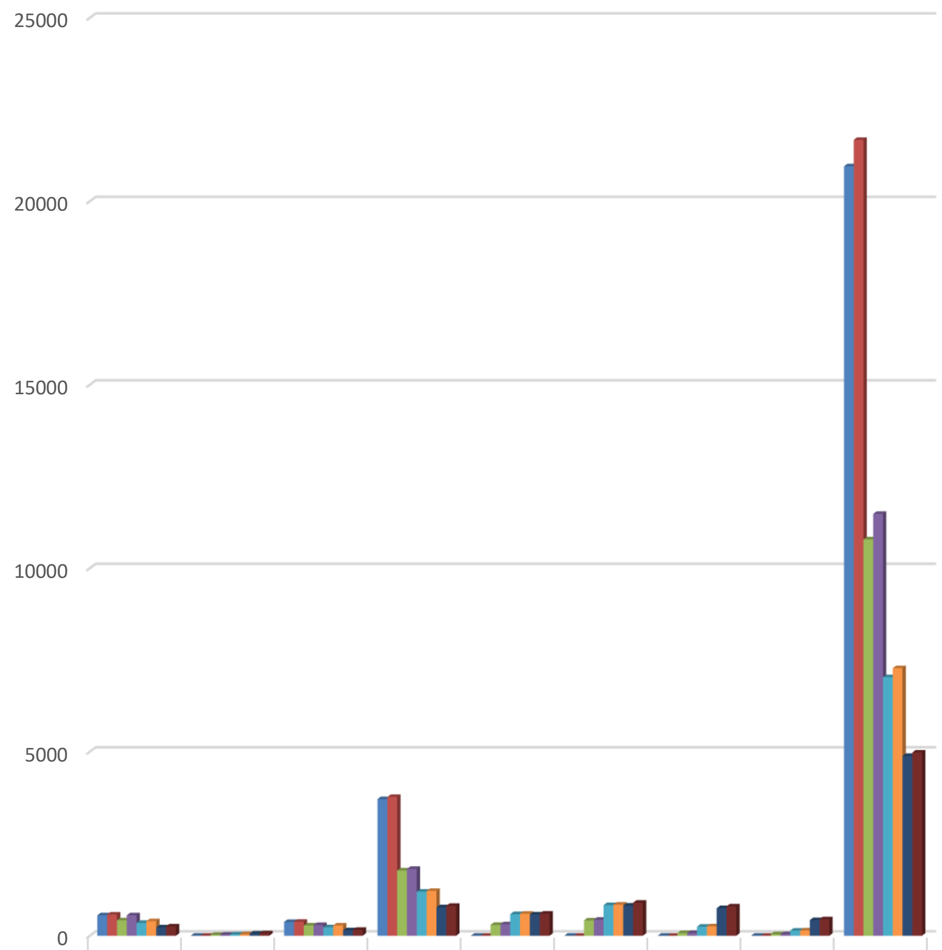

	∑Ploss (kW)	% Ploss Reduction	∑Qloss (kVAr)	∑ Purchased	WTinstallationcost ($) x105	WTO&Mcost($) x105	PVinstallationcost ($) x105	PV O&Mcost($) x105	∑Emission (lb/kWh)
Cases 1 CSA	554,55	0	371,87	3706,25	0	0	0	0	20952
Cases 1 HBA	575,21	0	379,15	3766,58	0	0	0	0	21672
Cases 2 CSA	419,7	24,32	279,45	1772,06	293,1	415,28	73,61	41,72	10786,2
Cases 2 HBA	554,3	32,12	290,14	1814,14	310,14	435,54	75,25	43,21	11482,2
Cases 3 CSA	348,57	37,14	228,85	1196,23	586,21	830,56	245,55	139,16	7030,67
Cases 3 HBA	395,49	42,14	278,85	1215,54	598,37	843,94	256,32	143,58	7274,75
Cases 4 CSA	225,81	59,28	148,9	772,78	577,2	817,78	748,91	424,42	4884,5
Cases 4 HBA	251,94	66,14	161,27	812,36	599,12	895,55	797,48	447,25	4976,45

Figure4.15. The results of all cases before and after DERs integration.

The comparisons result obtains from the HBA and CSA for the Real power loss during 24 hours after DERs integration, Reactive power loss during 24 hours after DERs integration, purchase active power cost from grid during 24 hours after DERs integration, Voltage deviation during 24 hours after DERs integration for all cases shown in figure 4.16.

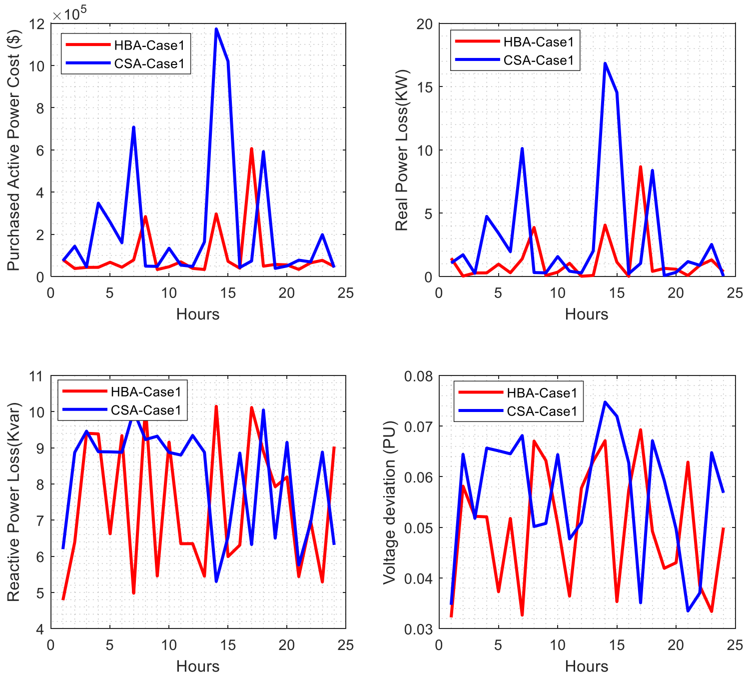
×10^5
Purchased Active Power Cost ($)
HBA-Case1
CSA-Case1
Hours
Real Power Loss(KW)
HBA-Case1
CSA-Case1
Hours
Reactive Power Loss(Kvar)
HBA-Case1
CSA-Case1
Hours
Voltage deviation (PU)
HBA-Case1
CSA-Case1
Hours

(a)

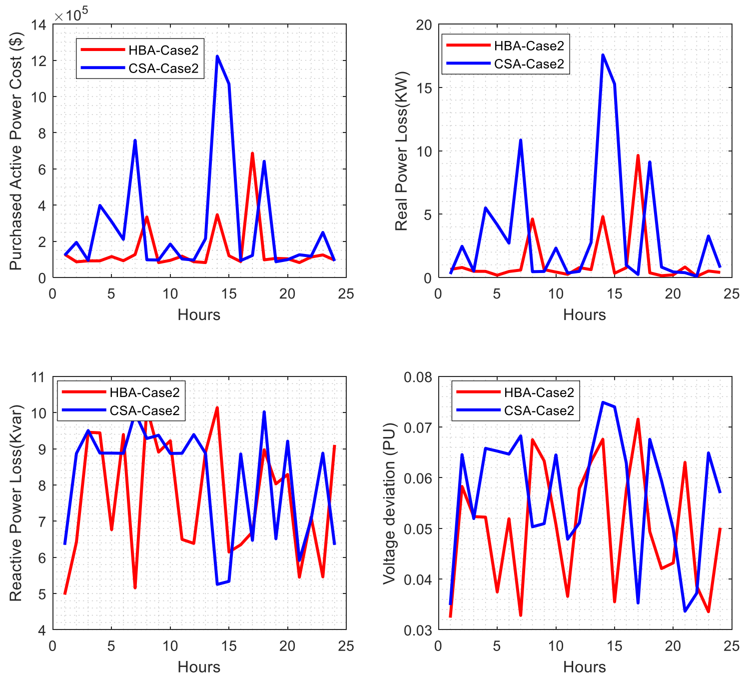
×10^5
Purchased Active Power Cost ($)
HBA-Case2
CSA-Case2
Hours
Real Power Loss(KW)
HBA-Case2
CSA-Case2
Hours
Reactive Power Loss(Kvar)
HBA-Case2
CSA-Case2
Hours
Voltage deviation (PU)
HBA-Case2
CSA-Case2
Hours

(b)

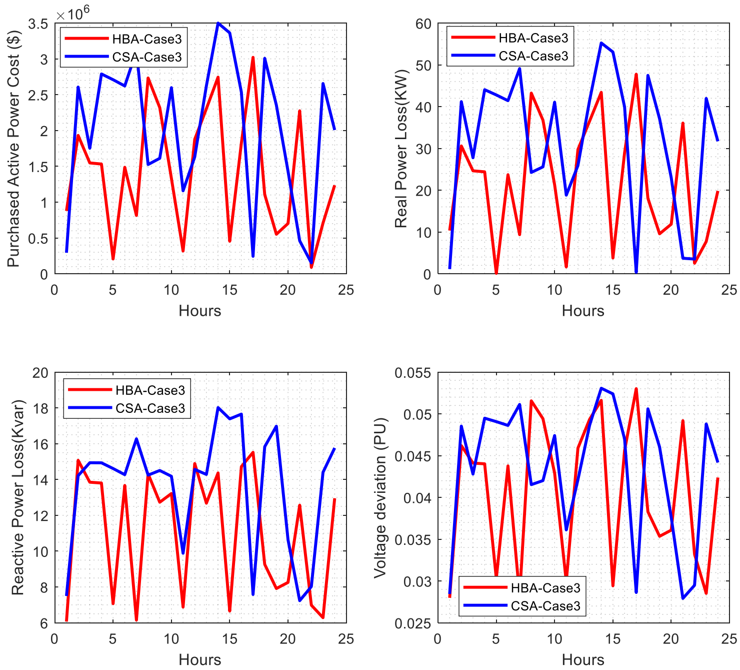

(c)

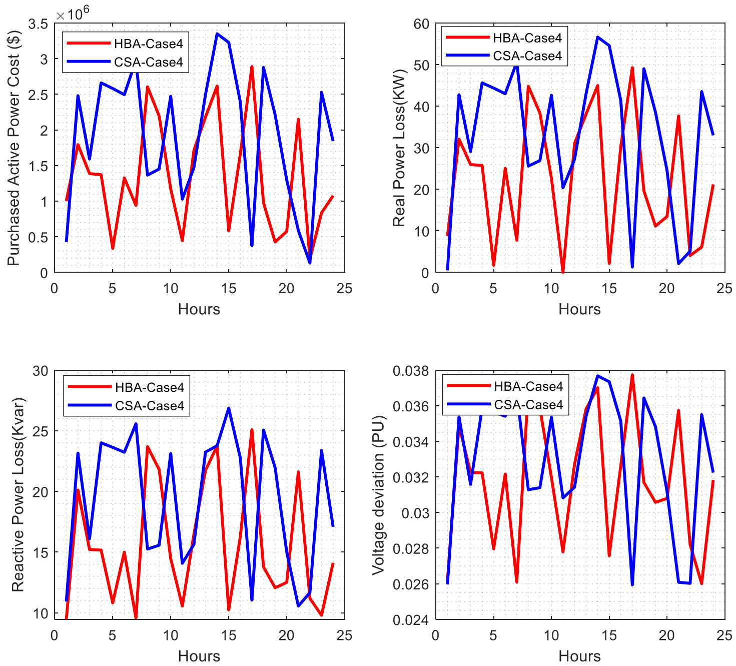

(d)

Figure 4.16. Active power loss during 24 hours after DERs integration, Reactive power loss during 24 hours after DERs integration, Purchase active power cost from grid during 24 hours after DERs integration, Voltage deviation during 24 hours after DERs integration, a) Case 1, b) Case 2, c) Case 3, d) Case 4.

In this thesis four scenario with honey-bee colony and crow search algorithm are implemented and tested. From the results it can be understand that the power loss value in case 1 for the CSA and HBA are reached to 554.55 (kW) and 575.21 (kW) respectively. That's mean the CSA has low power loss that the HBA. Also, for other cases we have reached low power loss in CSA method than the HBA. For the wind turbine installation cost in case 1 we didn't use this energy station, however in case 2 we reached to 293.1 (kW) and 310.14 (kW) from the CSA and HBA respectively. For other cases also this installation cost is low in the CSA. As the comparison results that illustrated in figure 4.15 it can be understand that the CSA has low cos than the HBA. We can understand that the CSA has more efficient results and it can find the parameter better that the HBA.

The statistical test results are shown in table 4.4.

Table 4.4. Statistical results.

Statistical parameter	CSA Algorithm	HBA Algorithm
Average Value	3125	3251
Standard Deviation	12.5	16.2
Best Fitness	3000	3215
Worst Fitness	5000	5654
Number of trials	100	100

Also following figure shows the graphical illustration.

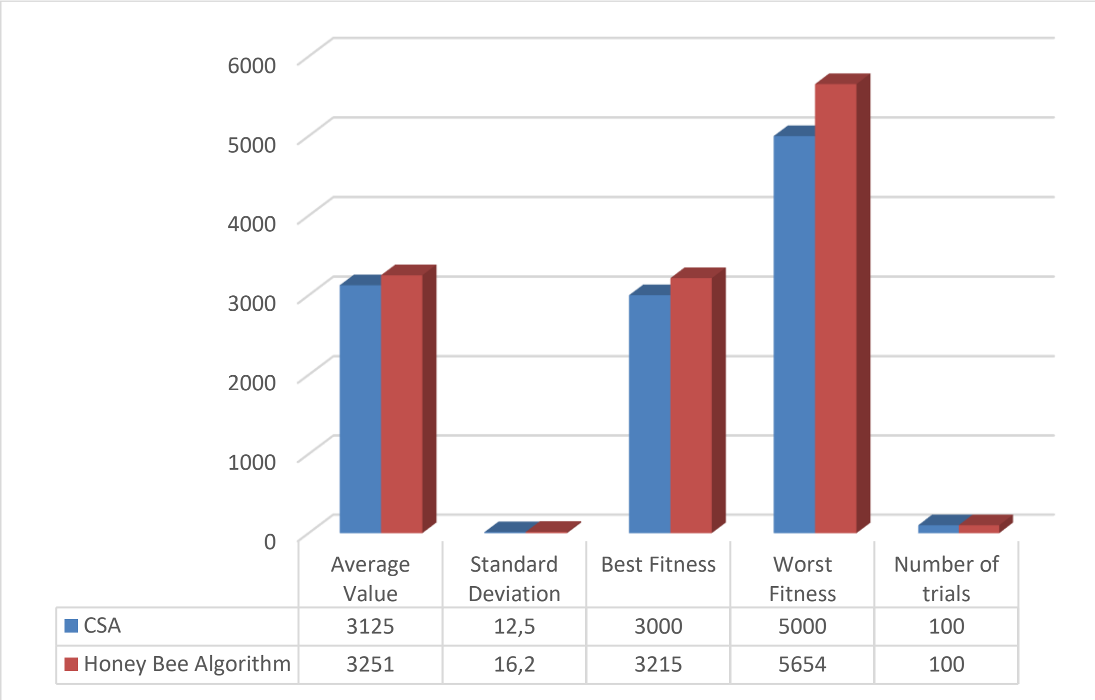

	Average Value	Standard Deviation	Best Fitness	Worst Fitness	Number of trials
CSA	3125	12,5	3000	5000	100
Honey Bee Algorithm	3251	16,2	3215	5654	100

Figure 4.17. Statistical results between (CSA) and (HBA)

CHAPTER 5

CONCLUSION AND FUTURE WORKS

5.1. CONCLUSION

In traditional transmission and distribution networks, the energy required for many residential, commercial, and industrial sites was provided through large sources. Some of these consumers were located near concentrated power plants, while some were further away and sometimes much, much further away.

Conversely, in Distributed Energy Generation (DG), the system has smaller, decentralized resources that generate electricity at a much closer distance to consumers. In this type of system, there are many manufacturers and although they have less production alone, but all of them are connected to the network and will be much more effective with each other.

Several technologies form the backbone of the DG system. The most prominent of these are solar, wind and hydropower technology. Another technology is cogeneration technology, which arises from the energy residues of other technologies. Simultaneous generation technology is an energy storage system that is connected to the grid and retains energy for as long as needed.
Imagine for a second you were transposed into the karmic driven world of Earl. Imagine for a second you were transposed into the karmic driven world of Earl. Towers may be bulky and powerful, but you may not always be as confident as you are now. The reasons must be clear. With a network of smaller, more uniformly distributed towers, your operator can provide the best possible service to its customers.

Some of this energy is wasted when centralized power plants transfer energy to remote locations. In DG distributed generation systems, energy generators are closer to consumers, so energy wasted is reduced and productivity is increased. In the old methods of energy distribution, a defect in any part of the system means that everyone is harmed, which in the new system is less likely to happen.

In the event of a natural disaster, DG can be used as an emergency resource for public services. By generating localized energy, DG systems reduce energy demand and reduce congestion in the main grid during peak energy consumption in certain areas.

Finally, it is environmentally beneficial because the distributed energy tends to be renewable. More use of renewable resources means less destruction and less destruction means the earth becomes a happier place for all of us.

In this thesis, relative analysis of techno-economic viability with DERs on distribution system has been considered. Consequently, a new multi objective function is designed. This objective function is minimized successfully through population-based CSA optimization algorithm. In addition, identify the optimal locations along with the optimum quantity of DERs in distribution system simultaneously. Thus, it achieves optimum result under load improbability state. The following points have been summarized from this very important study.

- Shared effects of DERs on distribution system have been examined. It is noticed that, after DERs integration the entire total expenses, power loss, voltage deviation, emission level and energy cost of the EVs get reduced appreciably.

- Weibull and beta PDF have been utilized successfully for evaluating the probability values of wind speed and solar irradiance for each hour respectively. These probability values are helpful to determine the EOP. Then, search out the optimum number of WT units and PV-modules accordingly.

- In this work, the renewable power sources operated at different power factor such as unity, 0.95 lagging/leading. If these renewable power sources operated at 0.95 lagging power factor, it seems that the test network generates better results.

- With EVs, vehicle owner's performance of discharging/charging their EVs for receiving financial advantages may increase the load demand during off-peak hours of the grid.

The achieved simulation outcomes through CSA algorithm are competent and adequate for solving more typical optimization tasks. In addition, it also experienced that the algorithm is efficient and capable to search out the optimum result in fewer number of cycles.

In this thesis, relative analysis of techno-economic viability with DERs on distribution system has been considered. Consequently, a new multi objective function is designed. This objective function is minimized successfully through population-based Bee Colony optimization algorithm. In addition, identify the optimal locations along with the optimum quantity of DERs in distribution system simultaneously. Thus, it achieves optimum result under load improbability state.

5.2. FUTURE WORKS

In future we can use the other meta-heuristic methods and artificial intelligence to improve the performance of the system. Also, a comprehensive energy management model can be proposed to operate a modified distribution system, considering smart homes. In that model, smart home subscribers can participate in a load accountability program and the subscriber is considered as a key constraint. The model also can be considering uncertainties in the amount of load demand, the amount of renewable energy production and the price of electricity. The Monte Carlo simulation method can use to generate the scenarios and the metaheuristic algorithm can be used to reduce their number. To approximate the simulation conditions to the actual operating conditions, the model of seasonal changes in demand and production is considered and the operation problem can be solved.

REFERENCES

1. Pepermans, G., Driesen, J., Haeseldonckx, D., Belmans, R., and D’haeseleer, W., "Distributed generation: definition, benefits and issues", ***Energy Policy***, 33 (6): 787–798 (2005).

2. Arfeen, Z. A., Khairuddin, A. B., Larik, R. M., and Saeed, M. S., "Control of distributed generation systems for microgrid applications: A technological review", ***International Transactions On Electrical Energy Systems***, 29 (9): e12072 (2019).

3. ÖZCAN, E. C. and Serpil, E., "TÜRKİYE’DE ELEKTRİK ÜRETİM PLANLAMASI İÇİN ÇOK AMAÇLI BİR KARIŞIK TAM SAYILI DOĞRUSAL PROGRAMLAMA MODELİ", ***Selçuk Üniversitesi Mühendislik, Bilim Ve Teknoloji Dergisi***, 1 (1): 41–54 (2008).

4. Ramanathan, R. and Ganesh, L. S., "Energy alternatives for lighting in households: an evaluation using an integrated goal programming-AHP model", ***Energy***, 20 (1): 63–72 (1995).

5. Boot, P. A. and Van Bree, B., "A Zero-Carbon European Power System in 2050: Proposals for a Policy Package", ***ECN, Energy Research Centre Of The Netherlands***, (2010).

6. Parks, K., Denholm, P., and Markel, T., "Costs and emissions associated with plug-in hybrid electric vehicle charging in the Xcel Energy Colorado service territory", ***National Renewable Energy Lab.(NREL), Golden, CO (United States)***, (2007).

7. Marshall, B. M., Kelly, J. C., Lee, T.-K., Keoleian, G. A., and Filipi, Z., "Environmental assessment of plug-in hybrid electric vehicles using naturalistic drive cycles and vehicle travel patterns: A Michigan case study", ***Energy Policy***, 58: 358–370 (2013).

8. Afsharzade, N., Papzan, A., Ashjaee, M., Delangizan, S., Van Passel, S., and Azadi, H., "Renewable energy development in rural areas of Iran", ***Renewable And Sustainable Energy Reviews***, 65: 743–755 (2016).

9. Pacesila, M., Burcea, S. G., and Colesca, S. E., "Analysis of renewable energies in European Union", ***Renewable And Sustainable Energy Reviews***, 56: 156–170 (2016).

10. Islam, M. M., Mun, H., Bostami, A. B. M. R., Park, K., and Yang, C., "Combined active solar and geothermal heating: A renewable and environmentally friendly energy source in pig houses", ***Environmental Progress & Sustainable Energy***, 35 (4): 1156–1165 (2016).

11. Iqbal, M., Azam, M., Naeem, M., Khwaja, A. S., and Anpalagan, A., "Optimization classification, algorithms and tools for renewable energy: A review", ***Renewable And Sustainable Energy Reviews***, 39: 640–654 (2014).

12. Nasiraghdam, H. and Jadid, S., "Optimal hybrid PV/WT/FC sizing and distribution system reconfiguration using multi-objective artificial bee colony (MOABC) algorithm", ***Solar Energy***, 86 (10): 3057–3071 (2012).

13. Kayal, P. and Chanda, C. K., "A multi-objective approach to integrate solar and wind energy sources with electrical distribution network", ***Solar Energy***, 112: 397–410 (2015).

14. Gampa, S. R. and Das, D., "Optimum placement and sizing of DGs considering average hourly variations of load", ***International Journal Of Electrical Power & Energy Systems***, 66: 25–40 (2015).

15. Tan, S., Xu, J.-X., and Panda, S. K., "Optimization of distribution network incorporating distributed generators: An integrated approach", ***IEEE Transactions On Power Systems***, 28 (3): 2421–2432 (2013).

16. Yang, H.-T. and Liao, J.-T., "MF-APSO-based multiobjective optimization for PV system reactive power regulation", ***IEEE Transactions On Sustainable Energy***, 6 (4): 1346–1355 (2015).

17. Tolabi, H. B., Ali, M. H., and Rizwan, M., "Simultaneous reconfiguration, optimal placement of DSTATCOM, and photovoltaic array in a distribution system based on fuzzy-ACO approach", ***IEEE Transactions On Sustainable Energy***, 6 (1): 210–218 (2014).

18. Wen, S., Lan, H., Fu, Q., David, C. Y., and Zhang, L., "Economic allocation for energy storage system considering wind power distribution", ***IEEE Transactions On Power Systems***, 30 (2): 644–652 (2014).

19. Hung, D. Q., Mithulananthan, N., and Lee, K. Y., "Determining PV penetration for distribution systems with time-varying load models", ***IEEE Transactions On Power Systems***, 29 (6): 3048–3057 (2014).

20. Teng, J.-H., Luan, S.-W., Lee, D.-J., and Huang, Y.-Q., "Optimal charging/discharging scheduling of battery storage systems for distribution systems interconnected with sizeable PV generation systems", ***IEEE Transactions On Power Systems***, 28 (2): 1425–1433 (2012).

21. Senthil kumar, J., Charles Raja, S., Srinivasan, D., and Venkatesh, P., "Hybrid renewable energy-based distribution system for seasonal load variations", ***International Journal Of Energy Research***, 42 (3): 1066–1087 (2018).

22. Khatod, D. K., Pant, V., and Sharma, J., "Evolutionary programming based optimal placement of renewable distributed generators", ***IEEE Transactions On Power Systems***, 28 (2): 683–695 (2012).

23. Atwa, Y. M. and El-Saadany, E. F., "Probabilistic approach for optimal allocation of wind-based distributed generation in distribution systems", ***IET Renewable Power Generation***, 5 (1): 79–88 (2011).

24. Atwa, Y. M. and El-Saadany, E. F., "Optimal allocation of ESS in distribution systems with a high penetration of wind energy", ***IEEE Transactions On Power Systems***, 25 (4): 1815–1822 (2010).

25. Atwa, Y. M., El-Saadany, E. F., Salama, M. M. A., and Seethapathy, R., "Optimal renewable resources mix for distribution system energy loss minimization", ***IEEE Transactions On Power Systems***, 25 (1): 360–370 (2009).

26. Suganya, S., Charles Raja, S., and Venkatesh, P., "Smart management of distinct plug-in hybrid electric vehicle charging stations considering mobility pattern and site characteristics", ***International Journal Of Energy Research***, 41 (14): 2268–2281 (2017).

27. Kayal, P. and Chanda, C. K., "Optimal mix of solar and wind distributed generations considering performance improvement of electrical distribution network", ***Renewable Energy***, 75: 173–186 (2015).

28. Niknam, T., Fard, A. K., and Seifi, A., "Distribution feeder reconfiguration considering fuel cell/wind/photovoltaic power plants", ***Renewable Energy***, 37 (1): 213–225 (2012).

29. Niknam, T., Kavousifard, A., Tabatabaei, S., and Aghaei, J., "Optimal operation management of fuel cell/wind/photovoltaic power sources connected to distribution networks", ***Journal Of Power Sources***, 196 (20): 8881–8896 (2011).

30. Rabiee, A. and Mohseni-Bonab, S. M., "Maximizing hosting capacity of renewable energy sources in distribution networks: A multi-objective and scenario-based approach", ***Energy***, 120: 417–430 (2017).

31. Kefayat, M., Ara, A. L., and Niaki, S. A. N., "A hybrid of ant colony optimization and artificial bee colony algorithm for probabilistic optimal placement and sizing of distributed energy resources", ***Energy Conversion And Management***, 92: 149–161 (2015).

32. Möllerström, E., Gipe, P., Beurskens, J., and Ottermo, F., "A historical review of vertical axis wind turbines rated 100 kW and above", ***Renewable And Sustainable Energy Reviews***, 105: 1–13 (2019).

33. Yang, D., Jin, Z., Zheng, T., and Jin, E., "An adaptive droop control strategy with smooth rotor speed recovery capability for type III wind turbine generators", ***International Journal Of Electrical Power & Energy Systems***, 135: 107532 (2022).

34. Wacker, B., Seebaß, J. V, and Schlüter, J. C., "A modular framework for estimating annual averaged power output generation of wind turbines", ***Energy Conversion And Management***, 221: 113149 (2020).

35. Campos, R. A., do Nascimento, L. R., and Rüther, R., "The complementary nature between wind and photovoltaic generation in Brazil and the role of energy storage in utility-scale hybrid power plants", ***Energy Conversion And Management***, 221: 113160 (2020).

36. Wollz, D. H., da Silva, S. A. O., and Sampaio, L. P., "Real-time monitoring of an electronic wind turbine emulator based on the dynamic PMSG model using a graphical interface", ***Renewable Energy***, (2020).

37. Zhang, J., Zhang, M., Li, Y., Qin, J., Wei, K., and Song, L., "Analysis of wind characteristics and wind energy potential in complex mountainous region in southwest China", ***Journal Of Cleaner Production***, 274: 123036 (2020).

38. Battaiotto, P. E., Mantz, R. J., and Puleston, P. F., "A wind turbine emulator based on a dual DSP processor system", ***Control Engineering Practice***, 4 (9): 1261–1266 (1996).

39. Chinchilla, M., Arnaltes, S., and Rodriguez-Amenedo, J. L., "Laboratory set-up for wind turbine emulation", (2004).

40. Arifujjaman, M., Iqbal, M. T., and Quaicoe, J. E., "An isolated small wind turbine emulator", (2006).

41. Li, W., Xu, D., Zhang, W., and Ma, H., "Research on wind turbine emulation based on DC motor", (2007).

42. Patel, R., Patki, C. V, and Agarwal, V., "Armature and field controlled DC motor based wind turbine emulation for wind energy conversion systems operating over a wide range of wind velocity", Sustainability in Energy and Buildings, ***Springer***, 117–125 (2009).

43. Mahdy, A., El-Hakim, S. M., and Hanafy, H. H., "Small wind turbine emulator with separately excited DC motor using analog electronic circuit", (2011).

44. Satpathy, A. S. and Sahoo, N. C., "Development of control scheme for a stand-alone wind system: Wind turbine emulated using DC motor", (2012).

45. Kouadria, S., Belfedhal, S., Berkouk, E. M., and Meslem, Y., "Development of real time wind turbine emulator based on DC motor controlled by PI regulator", (2013).

46. Martinez, F., Herrero, L. C., and de Pablo, S., "Open loop wind turbine emulator", ***Renewable Energy***, 63: 212–221 (2014).

47. Yadav, A. K., Singh, M., and Meena, D. C., "Modelling and simulation of wind turbine emulator using DC motor", (2016).

48. Bailapudi, M. P. K. and Sinha, N., "Fuzzy logic controlled wind turbine emulator (WTE)", (2016).

49. Benaaouinate, L., Khafallah, M., Mesbahi, A., and Martinez, A., "Development of a useful wind turbine emulator based on permanent magnet DC motor", (2017).

50. Sirouni, Y., El Hani, S., Naseri, N., Aghmadi, A., and El Harouri, K., "Design and Control of a Small Scale Wind Turbine Emulator with a DC Motor", (2018).

51. Moussa, I., Bouallegue, A., and Khedher, A., "New wind turbine emulator based on DC machine: Hardware implementation using FPGA board for an open-loop operation", ***IET Circuits, Devices & Systems***, 13 (6): 896–902 (2019).

52. Satish Kumar, P., Chandrasena, R. P. S., and Victor Sam Moses Babu, K., "Design and implementation of wind turbine emulator using FPGA for stand-alone applications", ***International Journal Of Ambient Energy***, 1–13 (2020).

53. Emna, M. E., Adel, K., and Mimouni, M. F., "The wind energy conversion system using PMSG controlled by vector control and SMC strategies", ***International Journal Of Renewable Energy Research (IJRER)***, 3 (1): 41–50 (2013).

54. Artyukhov, I. I., Stepanov, S. F., Molot, S. V, Tulepova, G. N., Erbaev, E. T., and Tulegenov, K. K., "Autonomous power supply system based on a diesel generator and renewable energy sources for remote rural areas", (2018).

55. Premkumar, K. and Manikandan, B. V, "Fuzzy PID supervised online ANFIS based speed controller for brushless dc motor", ***Neurocomputing***, 157: 76–90 (2015).

56. Premkumar, K. and Manikandan, B. V, "Bat algorithm optimized fuzzy PD based speed controller for brushless direct current motor", ***Engineering Science And Technology, An International Journal***, 19 (2): 818–840 (2016).

57. Premkumar, K. and Manikandan, B. V, "Stability and performance analysis of ANFIS tuned PID based speed controller for brushless DC motor", ***Current Signal Transduction Therapy***, 13 (1): 19–30 (2018).

58. Premkumar, K. and Manikandan, B. V, "Online Fuzzy Supervised Learning of Radial Basis Function Neural Network Based Speed Controller for Brushless DC Motor", Power Electronics and Renewable Energy Systems, ***Springer***, 1397–1405 (2015).

59. Premkumar, K. and Manikandan, B. V, "GA-PSO optimized online ANFIS based speed controller for Brushless DC motor", ***Journal Of Intelligent & Fuzzy Systems***, 28 (6): 2839–2850 (2015).

60. Prem Kumar, K., Thamizhselvan, T., Priya, M. V., Carter, S. B. R., and Sivakumar, L. P., "Fuzzy anti-windup PID controlled induction motor", ***Int J Eng Adv Technol***, 9 (1): 184–189 (2019).

61. Thamizhselvan, T., Seyezhai, R., and Premkumar, K., "Maximum power point tracking algorithm for photovoltaic system using supervised online coactive neuro fuzzy inference system", ***Journal Of Electrical Engineering***, 17 (1): 270–286 (2017).

62. Hepzibah, A. A. and Premkumar, K., "ANFIS current–voltage controlled MPPT algorithm for solar powered brushless DC motor based water pump", ***Electrical Engineering***, 102 (1): 421–435 (2020).

63. Shyam, D., Premkumar, K., Thamizhselvan, T., Nazar Ali, A., and Vishnu Priya, M., "Symmetrically modified laddered H-bridge multilevel inverter with reduced configurational parameters", ***International Journal Of Engineering And Advanced Technology***, 9 (1): 5525–5532 (2019).

64. Hawkes, A. D. and Leach, M. A., "Modelling high level system design and unit commitment for a microgrid", ***Applied Energy***, 86 (7–8): 1253–1265 (2009).

65. Morais, H., Kádár, P., Faria, P., Vale, Z. A., and Khodr, H. M., "Optimal scheduling of a renewable micro-grid in an isolated load area using mixed-integer linear programming", ***Renewable Energy***, 35 (1): 151–156 (2010).

66. Mohamed, F. A. and Koivo, H. N., "Microgrid online management and balancing using multiobjective optimization", (2007).

67. Costa, P. M. and Matos, M. A., "Assessing the contribution of microgrids to the reliability of distribution networks", ***Electric Power Systems Research***, 79 (2): 382–389 (2009).

68. Costa, P. M. and Matos, M. A., "Economic analysis of microgrids including reliability aspects", (2006).

69. Guo, Q., Pan, Y., Zhou, Q., Zhang, C., and Bi, Y., "Kinetic Energy Calculation in Granite Particles Comminution Considering Movement Characteristics and Spatial Distribution", ***Minerals***, 11 (2): 217 (2021).

70. Xu, B., Zhang, J., Egusquiza, M., Chen, D., Li, F., Behrens, P., and Egusquiza, E., "A review of dynamic models and stability analysis for a hydro-turbine governing system", ***Renewable And Sustainable Energy Reviews***, 144: 110880 (2021).

71. Domnikov, A. and Khodorovsky, M., "Methodological approach to the research of energy cogeneration systems operational reliability indicators", ***International Journal Of Energy Production And Management***, 6 (3): 263–276 (2021).

72. Bhatti, G., Mohan, H., and Singh, R. R., "Towards the future of ssmart electric vehicles: Digital twin technology", ***Renewable And Sustainable Energy Reviews***, 141: 110801 (2021).

73. Naderipour, A., Abdul-Malek, Z., Hajivand, M., Seifabad, Z. M., Farsi, M. A., Nowdeh, S. A., and Davoudkhani, I. F., "Spotted hyena optimizer algorithm for capacitor allocation in radial distribution system with distributed generation and microgrid operation considering different load types", ***Scientific Reports***, 11 (1): 1–15 (2021).

74. Dileep, G., "A survey on smart grid technologies and applications", ***Renewable Energy***, 146: 2589–2625 (2020).

75. Nair, R. P., "A Proposed System for a Smart Grid Implementation at Oklahoma State University", ***Oklahoma State University***, (2011).

76. Dixit, M., Kundu, P., and Jariwala, H. R., "Incorporation of distributed generation and shunt capacitor in radial distribution system for techno-economic benefits", ***Engineering Science And Technology, An International Journal***, 20 (2): 482–493 (2017).

77. Black, V., "Cost and performance data for power generation technologies", ***Prepared For The National Renewable Energy Laboratory***, (2012).

78. Maleki, A., Khajeh, M. G., and Ameri, M., "Optimal sizing of a grid independent hybrid renewable energy system incorporating resource uncertainty, and load uncertainty", ***International Journal Of Electrical Power & Energy Systems***, 83: 514–524 (2016).

79. Hu, W., Su, C., Chen, Z., and Bak-Jensen, B., "Optimal operation of plug-in electric vehicles in power systems with high wind power penetrations", ***IEEE Transactions On Sustainable Energy***, 4 (3): 577–585 (2013).

80. Saber, A. Y. and Venayagamoorthy, G. K., "Resource scheduling under uncertainty in a smart grid with renewables and plug-in vehicles", ***IEEE Systems Journal***, 6 (1): 103–109 (2011).

81. Boyle, G., "Renewable energy", ***Renewable Energy, By Edited By Godfrey Boyle, Pp. 456. Oxford University Press, May 2004. ISBN-10: 0199261784. ISBN-13: 9780199261789***, 456 (2004).

82. Ramelli, O., Saleh, S., and Stenflo, J., "Prospects of renewable energy in Libya", (2006).

83. Liang, S. and Zhu, J., "Dynamic Economic Dispatch of Microgrid with Biomass Power Generation", (2017).

84. Huang, Y., Zhang, J., Ann, F. T., and Ma, G., "Intelligent mixture design of steel fibre reinforced concrete using a support vector regression and firefly algorithm based multi-objective optimization model", ***Construction And Building Materials***, 260: 120457 (2020).

85. Karaboga, D. and Akay, B., "Artificial bee colony (ABC), harmony search and bees algorithms on numerical optimization", (2009).

86. Askarzadeh, A., "A novel metaheuristic method for solving constrained engineering optimization problems: crow search algorithm", ***Computers & Structures***, 169: 1–12 (2016).

87. Hinojosa, S., Oliva, D., Cuevas, E., Pajares, G., Avalos, O., and Gálvez, J., "Improving multi-criterion optimization with chaos: a novel Multi-Objective Chaotic Crow Search Algorithm", ***Neural Computing And Applications***, 29 (8): 319–335 (2018).

88. Karaboga, D., "An idea based on honey bee swarm for numerical optimization", ***Technical Report-Tr06, Erciyes University, Engineering Faculty, Computer …***, (2005).

89. Andrushia, A. D. and Patricia, A. T., "Artificial bee colony optimization (ABC) for grape leaves disease detection", ***Evolving Systems***, 11 (1): 105–117 (2020).

90. Dokeroglu, T., Sevinc, E., and Cosar, A., "Artificial bee colony optimization for the quadratic assignment problem", ***Applied Soft Computing***, 76: 595–606 (2019).

91. Teodorović, D., "Bee colony optimization (BCO)", Innovations in Swarm Intelligence, ***Springer***, 39–60 (2009).

92. Price, W. W., Taylor, C. W., and Rogers, G. J., "Standard load models for power flow and dynamic performance simulation", ***IEEE Transactions On Power Systems***, 10 (CONF-940702-): (1995).

93. Lopez, E., Opazo, H., Garcia, L., and Bastard, P., "Online reconfiguration considering variability demand: Applications to real networks", ***IEEE Transactions On Power Systems***, 19 (1): 549–553 (2004).

94. Ellis, A., Nelson, R., Von Engeln, E., Walling, R., McDowell, J., Casey, L., Seymour, E., Peter, W., Barker, C., and Kirby, B., "Reactive power interconnection requirements for PV and wind plants–recommendations to NERC", ***Sandia National Laboratories, Albuquerque, New Mexico***, 87185: (2012).

APPENDIX A

CODES

MATLAB codes

```
%CSA for CEED Optimization

close all; clear all; clc

%%%%%%%%%%%%%%%%%%%%%%%%%%%%%%%%%%
%%%%%%%%%%%%%%%%%%%%%%%%%%%%%%%
%%%%%%%%%

CostFunction=@(x) cost_HRESnew_monte1(x);      % Cost Function

nVar=8;            % Number of Decision Variables

pd=nVar;

VarSize=[1 nVar];   % Size of Decision Variables Matrix

VarMin=[50 1 0 0.5 0.5 0.5 0.5 0.5];         % Lower Bound of Variables

VarMax=[300 15 10 0.9 0.9 0.9 0.9 0.9];         % Upper Bound of Variables

% Number of Objective Functions

nObj=numel(CostFunction(unifrnd(VarMin,VarMax,VarSize)));

tmax=100;      % Maximum Number of Iterations

nPop=100;       % Population Size
```

```
%%%%%%%%%%%%%%%%%%%%%%%%%%%%%%%%%%%%%%%%%%%%%%%%%%%%%%%%%%%%%%%%%%%%%%%%%%%%%%%%%%%%%%%%%%%%%%%%%%%%%

% setting the CSA

LB =VarMin;   % Lower bound

UB = VarMax;  % Upper bound

%%pd=3; % Problem dimension (number of decision variables)

N=100; % Flock (population) size

AP=0.00001; % Awareness probability

fl=20; % Flight length (fl)

h1=52.03;

% [x]=init(N,pd); % Function for initialization

%

% xn=x;



for i=1:N
```

```
x(i,:)=unifrnd(VarMin,VarMax,VarSize);

F(i)=CostFunction(x(i,:)); % Function for fitness evaluation

end

%%%%%%%%%%%%%%%%%%%%%%%%%%%%%%%%%%%

function [ z ] = cost_HRESnew_monte1( x )

% HRES system consist of three component includ PV , Wind and diesel

% generator

%x=[100 3 1];x=[80 12 1];

c_unit=[340 16000 45000];%$

OM_cost=[3.4 165 4.5];% $/yr

M=[340 16000 45000];

k=[0 0 5];

F=sum(round([x(1) x(2) x(3)]).*(c_unit+M.*k+OM_cost));



% input parameter
```

```
n_montecarlo=100;

irradiation=zeros(24,n_montecarlo);

wind_power=zeros(24,n_montecarlo);

irradiation_ini=[0 0 0 0 0 0 0 0.083 0.18 0.18 0.23 0.22 0.53 0.33 0.3 0.13 0 0 0 0
    0,0,0,0]*3;

wind_power_ini=[0 0 0 0 0 0.5 0 0 0 0 1 4 9.2 10 9.4 10 9.2 3.3 0.5 3 0 0 0 0];

for t=1:24

  mu=wind_power_ini(t);

  wind_power(t,:)=normrnd(mu,0.05*mu,[1,n_montecarlo]);

end

for t=1:24

  mu=irradiation_ini(t);

  irradiation(t,:)=normrnd(mu,0.05*mu,[1,n_montecarlo]);

end
```

APPENDIX B

Journal

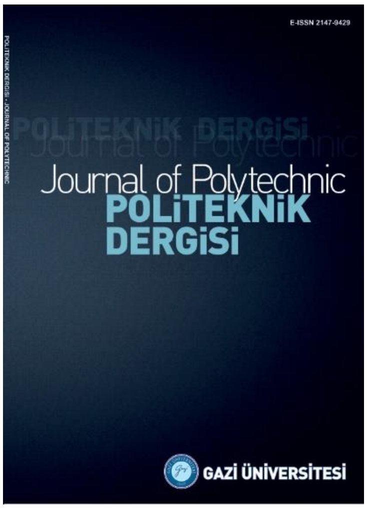

POLİTEKNİK DERGİSİ

JOURNAL of POLYTECHNIC

ISSN: 1302-0900 (PRINT), ISSN: 2147-9429 (ONLINE)

URL: http://dergipark.gov.tr/politeknik

The Techno-Economic and Environmental Analysis of a DER System in a Practical Radial Distribution Feeder under Load Uncertainty Conditions

Belirsiz Yük Koşullarında Bir DEK Sisteminin Pratik Radyal Dağıtımlı Besleyicide Tekno-Ekonomik ve Çevresel Analizi

Muhammet Tahir GÜNEŞER[1], Abdulbari Ali Mohamed FREI[2],

ORCID[1]: 0000-0003-3502-2034

ORCID[2]: 0000-0002-7134-2951

Bu makaleye şu şekilde atıfta bulunabilirsiniz(To cite to this article): FREI A. ve GÜNEŞER M. T., "The Techno-Economic and Environmental Analysis of a DER System in a Practical Radial Distribution Feeder under Load Uncertainty Conditions", *Politeknik Dergisi*, *(*): *, (*).
Erişim linki (To link to this article): http://dergipark.gov.tr/politeknik/archive DOI:

Conference papers

RESUME

Abdulbari Ali Mohamed FREI completed primary and elementary education in Mesallata, of Libya. In 2006, he graduated from Electrical and Electronic Engineering Department, Faculty of Engineering, from the Higher Institute for Comprehensive Professions Mesallata, after that, he worked as a full-time at the Higher Institute for Comprehensive Professions Mesallata in the period 2006 to up to now. In 2016, he got his MSc degree in Electrical and Electronic Engineering from Karabuk University-Turkey.

In 2016, he got his MSc degree in Electrical and Electronic Engineering from Karabuk University-Turkey. In 2017, he got a scholarship to continue his PhD education in Turkey. He started his PhD academic program at Karabuk University, registered in Department of Electrical and Electronic Engineering and started his PhD thesis research. His research area focuses on renewable energy systems.